Journal of Proteomics 128 (2015) 173–188

Contents lists available at ScienceDirect

Journal of Proteomics

journal homepage: www.elsevier.com/locate/jprot

Proteome and metabolome profiling of wild-type and *YCA1*-knock-out yeast cells during acetic acid-induced programmed cell death

Valentina Longo [a], Maša Ždralević [b,1], Nicoletta Guaragnella [b], Sergio Giannattasio [b], Lello Zolla [a,*], Anna Maria Timperio [a,*]

[a] Department of Ecology and Biology, "La Tuscia" University, Viterbo, Italy
[b] Institute of Biomembrane and Bioenergetics, CNR, Bari, Italy

ARTICLE INFO

Article history:
Received 19 May 2015
Received in revised form 3 July 2015
Accepted 5 August 2015
Available online 9 August 2015

Keywords:
Yeast
Programmed cell death
Acetic acid
Metacaspase
Proteomic
Metabolomic

ABSTRACT

Caspase proteases are responsible for the regulated disassembly of the cell into apoptotic bodies during mammalian apoptosis. Structural homologues of the caspase family (called metacaspases) are involved in programmed cell death in single-cell eukaryotes, yet the molecular mechanisms that contribute to death are currently undefined. Recent evidence revealed that a programmed cell death process is induced by acetic acid (AA-PCD) in *Saccharomyces cerevisiae* both in the presence and absence of metacaspase encoding gene *YCA1*. Here, we report an unexpected role for the yeast metacaspase in protein quality and metabolite control. By using an "omics" approach, we focused our attention on proteins and metabolites differentially modulated *en route* to AA-PCD either in wild type or *YCA1*-lacking cells. Quantitative proteomic and metabolomic analyses of wild type and *Δyca1* cells identified significant alterations in carbohydrate catabolism, lipid metabolism, proteolysis and stress-response, highlighting the main roles of metacaspase in AA-PCD. Finally, deletion of *YCA1* led to AA-PCD pathway through the activation of ceramides, whereas in the presence of the gene yeast cells underwent an AA-PCD pathway characterized by the shift of the main glycolytic pathway to the pentose phosphate pathway and a proteolytic mechanism to cope with oxidative stress.

Significance: The yeast metacaspase regulates both proteolytic activities through the ubiquitin–proteasome system and ceramide metabolism as revealed by proteome and metabolome profiling of *YCA1*-knock-out cells during acetic-acid induced programmed cell death.

1. Introduction

Apoptosis, the major form of programmed cell death (PCD) is a genetically regulated self-destruction program essential for both development and tissue homeostasis in multicellular organisms. PCD pathways are evolutionally conserved from yeast to mammals. Yeast *Saccharomyces cerevisiae* PCD shares both morphological and biochemical features with mammalian apoptosis, including chromatin condensation, externalization of phosphatidylserine onto the cell surface, DNA fragmentation as well as reactive oxygen species (ROS) accumulation and mitochondrial involvement [1,2]. Thus yeast has been used as a suitable model organism to investigate the cellular components and regulation of the PCD molecular machinery.

A characteristic feature of mammalian apoptosis is the activation of caspases. Caspases are endoproteases that hydrolyze peptide bonds in a reaction that depends on catalytic cysteine residues in the caspase active site and occurs only after certain aspartic acid residues in the substrate [3]. This group of proteolytic enzymes can be divided into two functional subgroups on the basis of their known or hypothetical roles. The first subgroup includes initiator or apical caspases (caspases 2, 8, 9 and 10) which are responsible for initiating caspase activation cascades, while the second subgroup composed by the downstream or effector caspases (caspases 3, 6 and 7) is responsible for the actual dismantling of the cell during apoptosis [4]. Deregulations of caspase protease expression or activity can lead to the development of several diseases, including cancer and neurodegenerative disorders [3].

Unlike mammals, yeast contains only one gene homologue of caspases, named *YCA1*, encoding for yeast metacaspase [5] which has substrate specificity different from canonical caspases and exhibits arginine/lysine-specific endopeptidase activities [6–9].

Recently, glyceraldehyde-3-phosphate dehydrogenase (GAPDH) has been identified as a common substrate of both yeast metacaspase and mammalian caspases [10]. However, most, but not all, yeast PCD pathways depend on the metacaspase Yca1p [11,12].

Acetic acid-induced PCD (AA-PCD) is a well-studied yeast PCD model characterized by early ROS accumulation and a major role played by mitochondria through release of cytochrome *c* (cyt c) accompanied

* Corresponding authors.
E-mail addresses: zolla@unitus.it (L. Zolla), timperio@unitus.it (A.M. Timperio).
[1] Present address: Institute for Research on Cancer and Aging, CNRS-UMR 7284-INSERM U1081, University of Nice Sophia-Antipolis, Nice, France.

http://dx.doi.org/10.1016/j.jprot.2015.08.003
1874-3919/

by respiratory chain defects (for refs see [13]). In particular, it has been shown that AA-PCD can occur *via* two alternative pathways, one activated in wild type (WT) cells, where cyt c is released, and the other which occurs in yeast cells lacking *YCA1* (*Δyca1*) without cyt c release [14,15].

Notably, an active proteolytic function of Yca1p in yeast PCD remains to be established [6,14]. On the other hand, the ability of metacaspase to both promote and antagonize different cell cycle checkpoints has been demonstrated, representing an early form of the proliferation/differentiation regulatory activity exhibited by metazoan caspases [16]. *YCA1* also contributes to the fitness and adaptability of growing yeast through clearance of insoluble protein aggregates [17,18] and has been implicated in the regulation of antioxidant status and mitochondrial respiration [15,19,20]. The concept of non-apoptotic roles of metacaspase has been expanded in our previous work in which we have performed a comparative analysis between wild type and *Δyca1* cells using combined proteomic and metabolomic approach. We have shown that the deletion of *YCA1* alters the carbon, amino acid and nucleotide metabolisms and interferes with protein biosynthesis and protein transport/folding. Moreover, in *YCA1*-knockout cells a stress response is activated [21].

A proteomic approach has already been used to investigate the mechanisms of yeast PCD triggered either by hydrogen peroxide [22] or by acetic acid [23]. In the present work, we extended this analysis by investigating the role of metacaspase *YCA1* in yeast AA-PCD through a combined proteomics and metabolomic analysis of either WT or *Δyca1* cells before and after acetic-acid treatment. Here we give new insights into the mechanism of yeast AA-PCD by analyzing the proteome and metabolome of acetic acid treated WT yeast cells in order to obtain more information about the proteins and, for the first time, metabolites involved in this process. The other aim of this study was the analysis of the effect of acetic acid treatment on *Δyca1* cells by performing a combined proteomics and metabolomic analysis. Finally, a comparison between WT and *Δyca1* cell AA-PCD was carried out to characterize the role of metacaspase in the PCD process. All analyses were carried out using cell treated with acetic acid for 150 min when maximum or no cyt *c* release occurs in WT or *Δyca1* cells, respectively [15,24].

2. Materials and methods

2.1. Yeast strains and plasmids

The yeast strains used in this study were W303-1B wild type (MATα ade2 leu2 his3 trp1 ura3) (WT) and W303-1B *yca1Δ::KanMX4* cells (*Δyca1*) [14]. Strains expressing mitochondria-targeted green fluorescence protein (mtGFP) have been prepared by transformation of either WT or *Δyca1* cells with plasmid pVT100U-mtGFP [25] (kindly provided by Dr. Ralf Braun, Universität Bayreuth, Bayreuth, Germany), using the one-step lithium acetate protocol [26] and selected on synthetic complete medium lacking uracil (SCD-ura).

2.2. Yeast growth/treatment conditions and protein extraction

Wild type and *Δyca1* yeast cells [14], were grown at 26 °C in 1% yeast extract, 2% peptone, 2% glucose (YPD) medium up to the exponential phase (OD_{600} about 0.7). An aliquot (Ctrl) (2×10^7 cells) was collected and used for proteomic analysis as a control before acetic acid treatment and the remainder was harvested, washed once and incubated in the same medium set to pH 3.00 with HCl in the presence of 80 mM acetic acid for AA-PCD induction [14]. Cells (2×10^7) were harvested after 150 min for further analysis.

Cycloheximide (Sigma-Aldrich) was added to yeast cell cultures grown to $OD_{600} = 0.5–0.6$ at a final concentration of 100 μg/mL and the culture was incubated for 30 min before acetic acid treatment which was then carried out in the presence of the same concentration of cycloheximide. Cell viability was determined by measuring colony-forming units (cfu) after 2 days of growth on YPD plates at 30 °C.

Proteins were extracted from either control or AA-PCD cells using YPX™ Yeast Protein Extraction Kit (Expedeon) as described in [21].

2.3. TUNEL assay and analysis of mitochondrial morphology

DNA fragmentation was detected in yeast cells by TUNEL assay (In Situ Cell Death Detection kit, fluorescein, Roche). AA-treated and control cells (2×10^7) were harvested at 150 min and before acetic acid treatment, respectively. Briefly, cells were fixed in 3.7% formaldehyde solution in PBS, digested with zymolyase and incubated in permeabilization solution (0.1% Triton-X-100, 0.1% sodium citrate) for 2 min on ice, and then with 30 μL TUNEL reaction mixture for 1 h at 37 °C. After incubation, cells were washed, resuspended in PBS and applied to microscopic slides and observed using a Leica TCS SP5 II microscope equipped with a laser-scanning confocal unit containing a He–Ne argon laser (Leica). Specimens were viewed through a Planapo 63X/1.25 oil immersion objective and images were acquired by LAS-AF version 2.2.1 build 4842 software.

To analyze mitochondrial morphology WT or *Δyca1* cells expressing mtGFP (WT-mtGFP and *Δyca1*-mtGFP, respectively) were each either grown on YPD to exponential phase ($OD_{600} \cong 0.7$) (control cells) or treated with acetic acid as described in Section 2.2 for 150 min. In either case 2 mL aliquots were withdrawn and cell pellet was resuspended in PBS and observed by confocal microscopy as above and images analyzed by ImageJ software.

2.4. 2D-SDS-PAGE

600 μg of proteins of each sample (Wt, *Δyca1* and Wt and *Δyca1* after acetic acid-induction) were precipitated adding a cold mix of tri-n-butyl phosphate/acetone/methanol (1:12:1) in ratio 1:4, in agitation for 90 min at 4 °C. Also, in this step lipid component of the samples was removed.

After high-speed centrifugation for 20 min, the pellets were dried and solubilized in the buffer containing 7 M urea, 2 M thiourea, 4% (w/v) CHAPS, 40 mM Tris–HCl and were reduced and alkylated, with 1,4-dithiothreitol (DTT) and iodoacetamide (IAA) respectively.

After precipitation, the pellets were solubilized and used to carry out passive rehydration of IPG strips (pH 3–10, non linear, 17 cm; Bio-Rad, CA, USA) over night.

Isoelectrofocusing (IEF) was performed on Protean IEF Cell (Bio-Rad, CA, USA) at 20 °C constant temperature and the total product time × voltage applied was 80,000 V-h.

SDS-PAGE was done in polyacrylamide gels (12% T, 2.6% C) at 35 mA per gel. The spots resulting by two-dimensional separation, were stained by sensitive Coomassie brilliant blue G-250 stain. For each sample, three technical replicates were performed.

2.5. Image analysis and statistics

Gels were imaged with ChemiDoc XRS + imaging system (Bio-Rad, CA, USA) and elaborated with ImageLab software (Bio-Rad, CA, USA).

Image analysis was carried out with computer software (Progenesis SameSpots, Version 2.0, Nonlinear Dynamics, Newcastle upon Tyne, UK). After manual and automatic alignment of twelve gels, the software generated a master list of detected spots and corresponding spot boundaries. For each protein spot, the average spot quantity value and its variance coefficient in each group was determined. One-way analysis of variance (ANOVA) was carried out at $p < 0.05$ to assess for absolute protein changes among the different treatments.

The statistically significant spots with fold ≥2 were cut by EXQuest Spot Cutter (Bio-Rad, CA, USA) and subjected to in-gel trypsin digestion.

2.6. Tryptic digestion

Protein spots observed in SDS-PAGE were carefully excised from Coomassie-stained polyacrylamide gels and subjected to in-gel trypsin digestion according to Shevchenko and coworkers [27] with minor modifications. The supernatant containing tryptic peptides was dried by vacuum centrifugation. Prior to mass spectrometric analysis, the peptide mixtures were redissolved in 10 μL of 5% formic acid (FA).

2.7. LC–ESI-CID–MS/MS (proteomic analysis)

Samples were analyzed using a split-free nano-flow liquid chromatography system (EASY-nLC II, Proxeon, Odense, Denmark) coupled with a 3D-ion trap (model AmaZon ETD, Bruker Daltonik, Germany) equipped with an online ESI nanosprayer (the spray capillary was a fused silica capillary, 0.090 mm O.D., 0.020 mm I.D.). For all experiments a sample volume of 15 μL was loaded by the autosampler onto a homemade 2 cm fused silica precolumn (100 mm I.D.; 375 mm O.D.; Reprosil C18-AQ, 5 mm, Dr Maisch GmbH, Ammerbuch-Entringen, Germany). Sequential elution of peptides was accomplished using a flow rate of 300 nL min 1 and a linear gradient from solution A (2% acetonitrile; 0.1% formic acid) to 50% of solution B (98% acetonitrile; 0.1% formic acid) in 40 min over the precolumn on-line with a homemade 15 cm resolving column (75 mm I.D.; 375 mm O.D. Reprosil C18-AQ 3 mm, Dr Maisch GmbH, Ammerbuch-Entringen, Germany). The acquisition parameters for the mass spectrometer were as follows: dry gas temperature, 220 °C; dry gas, 4.0 L min^{-1}; nebulizer gas, 10 psi; electrospray voltage, 4000 V; high-voltage end-plate offset, 200 V; capillary exit, 140 V; trap drive: 63.2; funnel 1 in. 100 V out 35 V and funnel 2 in. 12 V out 10 V; ICC target, 200 000; maximum accumulation time, 50 ms. The sample was measured with the "Enhanced Resolution Mode" at 8100 *m/z* per second (which allows mono isotopic resolution up to four charge stages) polarity positive, a scan range from *m/z* 300 to 1500, 5 spectra averaged, and rolling average of 1. The "Smart Decomposition" was set to "auto". Acquired CID spectra were processed in DataAnalysis 4.0, and deconvoluted spectra were further analyzed with BioTools 3.2 software and submitted to Mascot search program (in-house version 2.2, Matrix Science, London, UK). The following parameters were adopted for database searches: NCBInr database (release date 22/09/2012; 20 543 454 sequences; 7 050 788 919 residues); taxonomy = all entries; peptide and fragment mass tolerance of 0.3 Da; enzyme specificity trypsin with 2 missed cleavages considered; fixed modifications: carbamidomethyl (C); variable modifications: oxidation (M).

2.8. Sample preparation for metabolomic analysis

Wild type and *Δyca1* W303-1B yeast cells, grown in YPD medium up to the exponential phase (OD_{600} ≅0.7) (control cells) were harvested or incubated with acetic acid as described in section 2.2. Control cells or cells after acetic acid treatment (2×10^7 cells)were collected and used for metabolomic analysis. The yeast cells were resuspended in 100 μL of ice cold ultra-pure water (18 MΩ) to lyse the cells and then the tubes were plunged alternatively into a water bath at 37 °C for 0.5 min and at 4 °C for 0.5 min. To be sure that the cells are lysed, the samples were sonicated for 10 min. Samples were mixed with 400 μL of −20 °C methanol and then with 600 μL of −20 °C chloroform. The tubes were stored at −20 °C overnight. After centrifugation, we have taken the top fraction (methanol fraction) which contained metabolites and the bottom fraction (chloroform fraction) which contained lipids.

2.9. Rapid resolution reversed-phase HPLC

An Ultimate 3000 Rapid Resolution HPLC system (DIONEX, Sunnyvale, USA) was used to perform metabolite separation. The system featured a binary pump and vacuum degasser, well plate autosampler with a six-port micro-switching valve, and a thermostated column compartment. A Phenomenex Luna 3 μm HILIC 200A (150 × 2.0 mm) protected by a guard column HILIC 4 × 2.0 mm ID (Phenomenex) was used to perform metabolite separation over a phase B to phase A gradient lasting 35 min. For HILIC separation, 50 mM ammonium acetate was prepared by dissolving ammonium acetate in deionized water. The aqueous ammonium acetate was mixed with acetonitrile (95: 5, v/v). This was used for the mobile phase 'A'. Eluent 'B' was composed of a mixture of 50 mM aqueous ammonium acetate: water and acetonitrile (95:5, v/v).

Samples were loaded onto a Reprosil C18 column (2.0 mm × 150 mm, 2.5 mm—Dr Maisch, Germany) for metabolite separation.

Chromatographic separations were achieved at a column temperature of 30 1C; and a flow rate of 0.2 mL min^{-1}. For downstream positive ion mode (+) MS analyses, a 0–100% linear gradient of solvent A (ddH2O, 0.1% formic acid) to B (acetonitrile, 0.1% formic acid) was employed over 30 min, returning to 100% A in 2 min and a 6 min post-time solvent A hold. Acetonitrile, formic acid, and HPLC-grade water and standards (Ω 98% chemical purity) were purchased from Sigma Aldrich.

2.10. Mass spectrometry: Q-TOF settings

Due to the use of linear ion counting for direct comparisons against naturally expected isotopic ratios, time-of-flight instruments are most often the best choice for molecular formula determination. Thus, mass spectrometry analysis was carried out on an electrospray hybrid quadrupole time-of flight mass spectrometer MicroTOF-Q (Bruker-Daltonik, Bremen, Germany) equipped with an ESI-ion source. Mass spectra for metabolite extracted samples were acquired both in positive and negative ion modes. ESI capillary voltage was set at 4500 V (+) (−) ion mode. The liquid nebulizer was set to 27 psi and the nitrogen drying gas was set to a flow rate of 6 L min^{-1}. Dry gas temperature was maintained at 200°C. Data were stored in a centroid mode. Data were acquired with a stored mass range of *m/z* 50–1200. Calibration of the mass analyzer is essential in order to maintain a high level of mass accuracy. Instrument calibration was performed externally every day with a sodium formate solution consisting of 10 mM sodium hydroxide in 50% isopropanol: water, 0.1% formic acid. Automated internal mass scale calibration was performed through direct automated injection of the calibration solution at the beginning and at the end of each run by a 6-port divert-valve.

2.11. Data elaboration and statistical analysis

In order to reduce the number of possible hits in molecular formula generation, we exploited the SmartFormula3D TM software (Bruker Daltonics, Bremen, Germany), which directly calculates molecular formulae based upon the MS spectrum (isotopic patterns) and transition fingerprints (fragmentation patterns). This software generates a confidence-based list of chemical formulae on the basis of the precursor ions and all fragment ions, and the significance of their deviations to the predicted intact mass and fragmentation pattern. Triplicate runs for each one of the three biological replicates were exported as mzXML files and processed through MAVEN.52. Mass spectrometry chromatograms were elaborated for peak alignment, matching and comparison of parent and fragment ions, and tentative metabolite identification (within a 20 ppm mass-deviation range between observed and expected results against the imported KEGG database53) MAVEN is an open-source software that could be freely downloaded from the official project websites (http://genomics-pubs.princeton.edu/mzroll/index.php?show=download). Metabolite assignment was further elaborated in the light of the hydrophobicity/hydrophilicity of the compound and its relative retention time in the RP-HPLC run (as gleaned through database information and preliminary calibration with commercially-available ultra-pure standards, as previously described). Relative

quantitative variations of intact mass peak areas for each metabolite assigned through MS were normalized against internal standard.

3. Results

3.1. Acetic acid triggers PCD in both WT and Δyca1 cells

The main goal of this study was to determine the proteomic and metabolomic changes occurring *en route* to AA-PCD in either WT or *Δyca1* cells in order to identify the specific function/s of *YCA1* in the PCD pathways. Before starting the differential proteome and metabolome analysis, we aimed to confirm that both WT and *Δyca1* cells underwent an AA-PCD process as in [14]. Cell viability was analyzed as a function of time after acetic acid treatment of WT and *Δyca1* cells (Fig. 1A). At all times analyzed *Δyca1* cell viability was significantly higher than that of WT cells, showing a progressive decrease to 0% (WT) and 10% (*Δyca1*) at 200 min and death rates of $0.015 \pm 0.002\ min^{-1}$ and $0.007 \pm 0.002\ min^{-1}$ for WT and *Δyca1* cells, respectively [14]. The nature of cell death was confirmed by genomic DNA fragmentation analysis at 150 min, when the percentage of TUNEL positive cells was found to be about 50% for WT and 55% for *Δyca1* (Fig. 1B), with less than 5% TUNEL-positive control cells. The effect of protein synthesis inhibitor cycloheximide was also assessed on the viability of cells treated with acetic acid (Fig. 1C), showing a 45% (WT) and 40% (*Δyca1*) increase in cell viability as compared with untreated cells. Proteome and metabolome profiling was then performed with an equal amount of either cell types either before acetic acid treatment or after 150 min AA-PCD to determine the relative protein and metabolite changes *en route* to AA-PCD.

3.2. Differential proteomics and metabolomic analysis of either WT or Δyca1 AA-PCD cells

To compare the proteomic and metabolomic alterations caused by acetic acid treatment of either WT or *Δyca1* cells, all analyses were carried out using either cells treated with acetic acid for 150 min, when the maximum or no release of cyt c, respectively, occurs [15,24], or cells before acetic acid treatment as control.

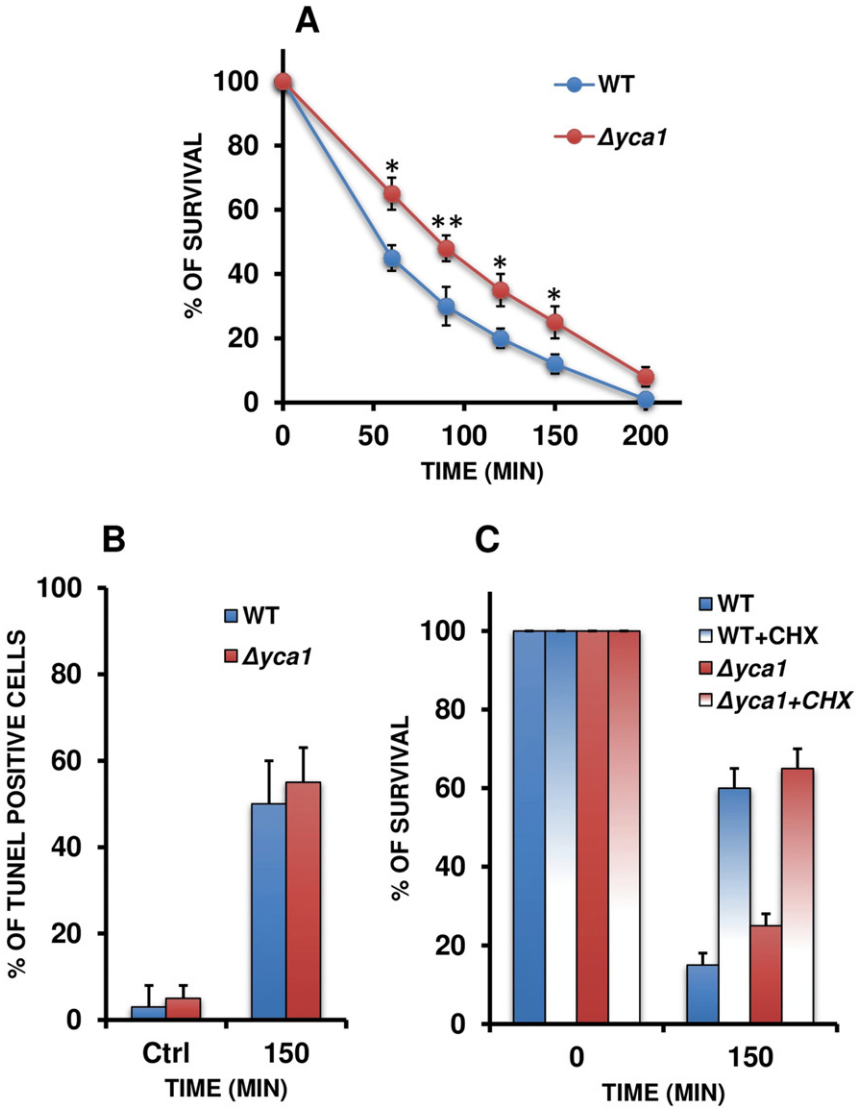

Fig. 1. Acetic acid triggers PCD in WT and *Δyca1* cells. WT and *Δyca1* cells, grown in YPD up to mid-log phase ($OD_{600} \cong 0.7$) (Ctrl), were treated with 80 mM acetic acid, at pH 3.00 and (A) cell viability was analyzed at indicated times by measuring colony-forming units (cfu) on YPD plates. (B) DNA fragmentation was analyzed by TUNEL assay in cells treated with acetic acid at 150 min or in control cells before acetic acid treatment. Percentage of TUNEL positive cells is reported. At least 400 cells were analyzed for each condition in three independent experiments. (C) Cell viability of acetic acid-treated cells was also analyzed both in the absence or the presence of cycloheximide at 150 min. 100% cell survival corresponds to cfu at time 0. The means of at least three independent experiments with standard errors are reported. Student's *t*-test: differences are statistically significant with $^{*}p < 0.05$ and $^{**}p < 0.01$ when comparing WT and *Δyca1* cells.

The analysis of protein expression in WT and *Δyca1* cells before and after 150 min of AA-PCD induction was performed by the extraction of total yeast soluble proteins and their subsequent resolution by 2-DE. The resulting Coomassie stained electropherograms were analyzed using Progenesis SameSpots software. Fig. 2 shows a typical image of 2-DE Coomassie-stained gel of WT (Fig. 2A) and *Δyca1* (Fig. 2B) cells where the spots affected by acetic acid treatment are marked by a symbol (+).

Comparison made between the total cellular proteome separated by 2-DE from AA-PCD WT cells at 150 min and the control cells before acetic acid treatment, resulted in the identification of 51 spots with altered expression (Fig. 2A). Only 8 spots (16%) were up-regulated; remaining 43 spots (84%) showed decreased expression caused by AA-treatment. These spots corresponded to the total of 45 proteins, that were classified into functional groups, as shown in Table 1 and Table 1S.

The same analysis made with *Δyca1* cells resulted in the identification of 52 protein spots with altered expression (see Fig. 2B). Only 10 spots (24%) were up-regulated; remaining 42 spots (76%) showed decreased expression caused by AA-treatment. These spots corresponded to the total of 47 proteins, that were classified into functional groups, as shown in Table 2 and Table 1S.

Total tandem-mass spectrometry-identified proteins, whose content was found to be changed after AA-PCD induction in either WT or *Δyca1* cells, were grouped in Fig. 3 using a Venn diagram and divided into three sets: the proteins which showed changes in their amount in both WT and *Δyca1* AA-PCD (A), only in WT cells (B) and only in *Δyca1* cells (C).

Metabolomic analyses were performed to integrate and expand the physiological and proteomics observations. Also in this case we compared WT and *Δyca1* cells before and after 150 min of AA-PCD induction. Due to the massive amount of output data, only significant results displaying absolute values for fold-change variations higher than 2.0 were reported along with feature number, feature name, p-value, mass to charge ratio (*m/z*), chromatographic retention times, day specific intensities and tentative identification (with isotope description, molecular weight deviation in ppm from database top hit reports, name, presence of K^+, Na^+, NH_4^+ adducts and MAVEN identifier), as identified by XCMS [28–31].

In order to report the main results in a more readable layout, metabolites accounting for the most relevant metabolic pathways were grouped and plotted as follows: metabolites involved in glycolysis, pentose phosphate pathway (PPP) and glutathione homeostasis (Fig. 4) and amino acid metabolism (Fig. 5). We could not detect intermediate metabolites of the Krebs cycle probably due to the unique glucose repression system that drastically suppresses respiration independently of oxygen availability in yeast growing in the presence of glucose as a sole carbon source [32].

In the following sections we will describe proteomics and metabolomics data separately for each group of proteins showing changes in their intracellular levels as reported in Fig. 3.

3.3. Proteins and metabolites found altered in both WT and Δyca1 AA-PCD cells

The proteins found altered in both WT and *Δyca1* AA-PCD cell analysis (Fig. 3, set A) are involved in several processes which are listed below.

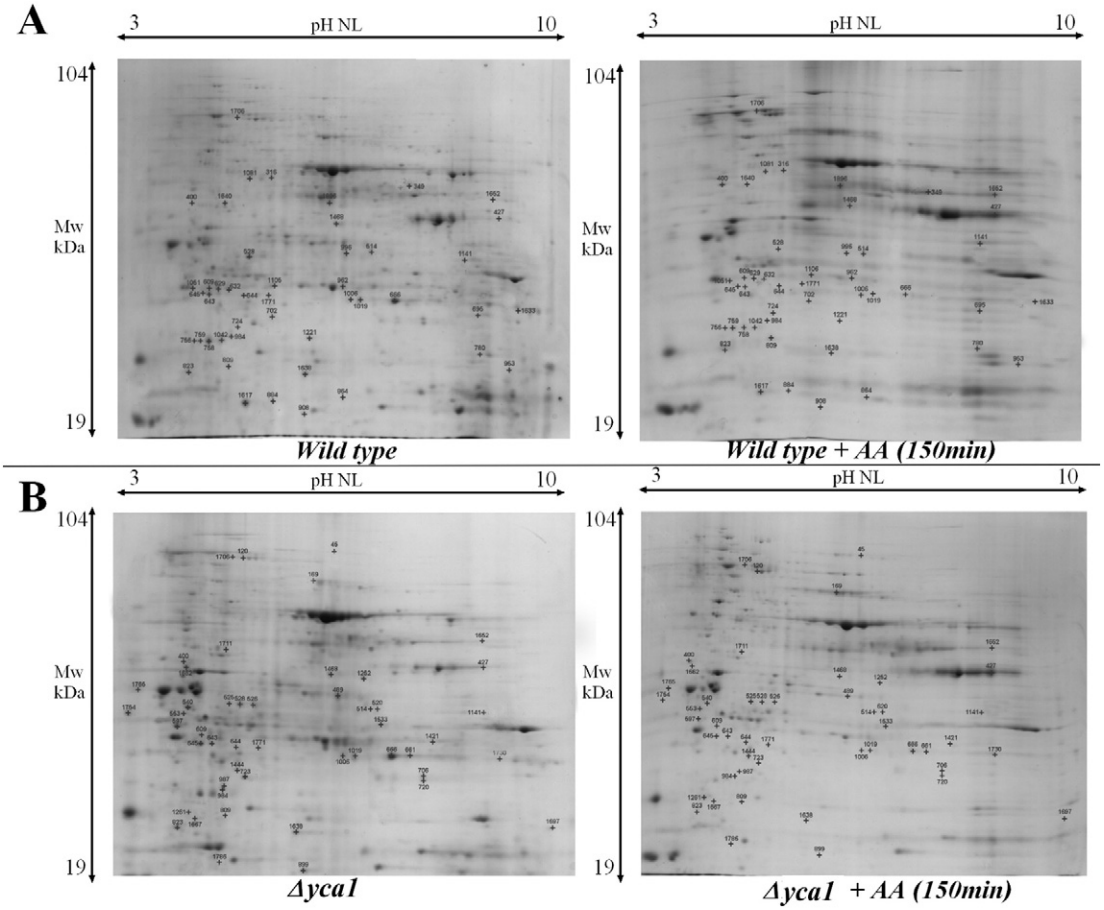

Fig. 2. Representative 2-DE gels (one of the 3 replicates) of total extract of wild type (panel A) or *Δyca1* (panel B) exponential-phase and AA-PCD (AA) W303-1B *Saccharomyces cerevisiae* cells. Statistically significant differential spots (p value < 0.05 and fold change > 2) for WT vs *Δyca1* analysis are shown in both panels. Molecular weight (MW) and pI range of the first dimension strips (3–10 NL) are indicated on the appropriate axis. Protein spot numbers are given as Table 1.

Table 1
Differentially expressed proteins in wild type AA-PCD.

Proteins identified	Biological protein function	NCBI accession number	Theoretical Mr (Da)	Theoretical pI	Spot number	No of peptides identified	Mascot score	Fold change	Expression level
Carbohydrate metabolism									
Eno1	Enolase I (phosphopyruvate hydratase)	gi|171455	46,830	6.16	1468	5	232	2.6	Down
Eno2	Enolase II	gi|6321968	46,942	5.67	528	19	957	3.6	Down
Hxk2	Hexokinase isoenzyme 2	gi|3710	27,525	5.19	1019	5	261	2.5	Down
Tdh3	Glyceraldehyde-3-phosphate dehydrogenase, isozyme 3	gi|45269553	35,780	6.72	1006	5	453	2.0	Down
					666	12	683	4.4	Down
Adh1	Alcohol dehydrogenase I	gi|223142	31,954	6.38	514	10	419	2.0	Down
		gi|6324486	37,282	6.21	349	18	827	2.6	Down
					996	13	589	2.7	Down
Fba1	Fructose 1,6-bisphosphate aldolase	gi|6322790	39,881	5.51	1896	4	120	2.7	Down
					1221 (fragment)	6	199	3.0	Down
Tpi1	Triose-phosphate isomerase	gi|6320255	26,893	5.74	1051	9	463	2.0	Down
Pdc1	Pyruvate decarboxylase	gi|871533	61,840	5.99	908 (fragment)	3	128	2.4	Down
		gi|256270485	46,909	5.74	1638 (fragment)	6	264	2.9	Down
		gi|259148033	61,719	5.71	702 (fragment)	4	177	2.1	Down
Pgk1	Phosphoglycerate kinase	gi|10383781	44,768	7.11	1771	14	667	2.0	Down
Amino acid metabolism									
Bat1	Mitochondrial branched-chain amino acid (BCAA) aminotransferase	gi|151944153	43,798	8.80	1652	2	97	2.3	Up
Ilv5	Isoleucine-plus-valine requiring	gi|323347291	44,510	9.1	1633	11	502	3.4	Down
Sam2	S-adenosylmethionine synthetase	gi|51013823	42,489	5.24	1081	7	284	2.2	Down
Nucleic acid metabolism									
Adk1	Adenylate kinase	gi|6320432	24,297	5.98	962	3	153	2.4	Down
Ura5	Uracil requiring	gi|6323530	24,763	5.80	962	3	127	2.4	Down
Ado1	Adenosine kinase	gi|6322565	36,521	4.99	1640	3	130	3.1	Down
Fur1	Uracil phosphoribosyltransferase	gi|171529	29,015	5.83	1105	12	736	2.7	Down
Transcription/translation machinery									
Eft2	Elongation factor 2 (EF-2)	gi|6320593	93,686	5.92	609 (fragment)	6	352	2.1	Down
Yef3	Yeast Elongation Factor	gi|173214	116,775	5.73	629 (fragment)	4	200	2.7	Down
Tif2	Translation initiation factor eIF4A	gi|6322323	44,840	5.02	1081	7	340	2.2	Down
Rpl12a	Ribosomal 60S subunit protein L12A	gi|6320781	17,869	9.43	953	5	341	2.6	Up
Rpl11b	Ribosomal 60S subunit protein L11B	gi|6321522	19,794	9.92	780	6	236	2.2	Up
Rps7a	Ribosomal Protein of the small subunit	gi|6324670	21,609	9.83	695	15	498	2.3	Up
Rps7b	Ribosomal Protein of the small subunit	gi|71064104	21,720	9.92	695	10	465	2.3	Up
Rpl8b	Ribosomal 60S subunit protein L8B	gi|6322984	28,151	10.02	1141	4	178	2.5	Up
Protein folding/degradation									
Ubc4	Ubiquitin-conjugating enzyme (E2)	gi|6319556	16,616	6.04	864	2	60	2.3	Up
Egd2	Enhancer of Gal4 DNA binding	gi|172043	18,295	4.84	756	3	141	2.2	Down
Stress response									
Ssa1	Stress-Seventy subfamily A Hsp70 family ATPase	gi|151941387	69,772	5.00	884 (fragment)	11	695	2.1	Down
Ssa2	Stress-Seventy subfamily A	gi|151941146	69,772	5.00	645 (fragment)	13	760	3.2	Down
		gi|151941387	69,772	5.00	643 (fragment)	12	710	2.8	Down
		gi|6323004	69,599	4.95	809 (fragment)	3	115	2.5	Down
					644 (fragment)	7	215	2.4	Down
Ssb1	Stress-Seventy subfamily B Hsp70 family ATPase	gi|6319972	66,732	5.32	632 (fragment)	7	296	2.1	Down
					1706	22	967	2.4	Up
Ssb2	Stress-Seventy subfamily B Hsp70 family ATPase SSB2	gi|151944335	66,669	5.32	632 (fragment)	7	296	2.1	Down
Sse1	ATPase component of the heat shock protein Hsp90 chaperone complex	gi|533365	77,647	5.12	400 (fragment)	4	260	2.2	Down
Zeo1	Zeocin resistance protein	gi|6324463	12,582	5.43	1617	9	376	2.3	Down
Hsp82	Hsp90 chaperone	gi|2624655	24,831	4.86	823	3	109	3.1	Down
Ahp1	Alkyl HydroPeroxide reductase	gi|6323138	19,274	5.01	1042	7	353	2.2	Down
					759	4	174	2.3	Down
					984	6	329	2.4	Down
					758	3	248	2.3	Down
Tsa1	Thioredoxin peroxidase	gi|6323613	21,690	5.03	984	3	95	2.4	Down
Hch1	High-Copy Hsp90 suppressor	gi|6324048	17,293	4.56	756	1	72	2.2	Down
Sis1	Type II HSP40 co-chaperone that interacts with the HSP70 protein Ssa1p	gi|6324321|	37,567	9.02	427	1	33		
Cell signaling									
Bmh1	Brain modulosignalin homologue 14-3-3 protein, major isoform	gi|671634	30,272	4.87	629	2	86	2.7	Down
Others									
Act1	Actin	gi|3328	41,907	5.53	316	12	558	2.0	Down
Vma1	Vacuolar membrane Atp-ase	gi|3417405	68,023	5.17	1706	15	691	2.4	Up
Tub1	alpha tubulin	gi|173058	50297	4.92	724 (fragment)	1	61	2.3	Down
Unknown									
Hmf1	Homologous Mmf1p factor	gi|398364461	14,011	5.28	1638	1	105	2.9	Down
Unidentified proteins									
682 604 1035 1016 913 1713 1157									Down

3.3.1. Carbohydrate metabolism

Except for pyruvate decarboxylase (Pdc1p), that showed increased or decreased expression in *Δyca1* or WT cells, respectively, all other enzymes involved in glycolysis/gluconeogenesis (Hxk2p, Fba1p, Tdh3p, Pgk1p, Eno1p, Eno2p, Adh1p) had a decreased expression en route to AA-PCD in both strains. Thus, there is a strong down-regulation of glycolytic enzymes in WT as well as in *Δyca1* cells en *route* to AA-PCD. Accordingly, metabolomic analysis reveals lower levels of several glycolytic intermediates (Fig. 4). Fructose-6-phosphate, fructose-1,6-bisphosphate, glyceraldehyde-3-phosphate, 2-phosphoglycerate and pyruvate decrease *en route* to AA-PCD. On the contrary, our metabolic data show an increase of PPP intermediates ribose 5-phosphate, sedoheptulose-7-phosphate and erythrose-4-phosphate, with a fold-increase in ribose 5-phosphate and sedoheptulose-7-phosphate significantly higher in WT than in *Δyca1* AA-PCD cells.

These results are in agreement with proteomic data of *S. cerevisiae* AA-treated BY4742 cells showing decreased expression of glycolytic enzymes [23].

3.3.2. Amino acid metabolism

Increased amount of branched-chain-amino-acid transaminase (Bat1p), a protein involved in leucine, isoleucine and valine synthesis [33] was found in either AA-PCD strains. It is of note that although, accordingly, leucine, isoleucine and valine, together with other eleven amino acids, accumulated in WT AA-PCD cells, a general amino acid depletion was found in *Δyca1* AA-PCD cells (Fig. 5).

3.3.3. Nucleotide metabolism

The amount of adenosine kinase (Ado1p) was found to be decreased in both WT and *Δyca1* cells. Ado1p catalyzes ATP dependent phosphorylation of purine nucleosides to monophosphate derivatives and, together with adenylate kinase (Adk1p), is involved in purine biosynthesis and salvage pathways. Ado1p is strictly required for the utilization of AdoMet and consequently adenosine, as a purine source [34]. In yeast, Ado1p does not seem to play a major role in adenine utilization, it is rather involved in recycling the adenosine produced through the methyl cycle [34].

3.3.4. Cell signaling

Brain modulosignalin homologue (Bmh1p), a yeast homologue of 14-3-3 protein, is the only protein involved in cell signaling found to be affected upon AA-PCD induction in both analyses and showed decreased expression upon AA-PCD. Bmh1p has a role in exocytosis, vesicle transport, Ras/MAPK signaling and rapamycin-sensitive signaling [35].

Deletion of the yeast Bmh1p was shown to extend chronological life span (CLS) by activating the stress response, protecting the cells from ROS-induced damages during chronological aging [36]. Thus, decreased expression of Bmh1p during WT and *Δyca1* AA-PCD could contribute to the overall higher susceptibility to oxidative stress *en route* to AA-PCD. Bmh1p has recently been shown to target misfolded proteins to aggresome, a key cytoplasmic organelle for sequestration and clearance of toxic protein aggregates [37], in agreement with a general decrease in heat-shock proteins *en route* to AA-PCD (see below).

3.3.5. Vacuolar acidification

Vma1p is the A subunit of the vacuolar membrane ATP-ase and contains the catalytic nucleotide binding site and it was found to be up-regulated both in WT and in *Δyca1* cells. Vacuolar ATP-ases are ATP-dependent proton pumps that acidify intracellular vacuolar compartments, important for many cellular processes, such as endocytosis, targeting of newly synthesized lysosomal enzymes, and other molecular targeting processes.

3.3.6. Stress response

Proteins involved in stress response consisted of Hsp70 and Hsp90 family proteins, as well as proteins involved in cell redox homeostasis (Ahp1p, Tsa1p) and cell wall stress response (Zeo1p). Four members of the Hsp70 family (Ssa1p, Ssa2p, Ssb1p, Ssb2p) showed decreased expression and fragmentation induced by AA-treatment with the exception of Ssb1p. The expression of Hsp90 chaperone family member, Hsp82p, a co-chaperone that regulates the activity of members of Hsp90 family, was found to decrease upon AA-treatment. Alkyl hydroperoxide reductase (Ahp1p) was identified in two different spots with similar Mr but different pI values, suggesting that some post-traslational modifications (PTMs) occurred; all of which down-regulated. The amount of Zeo1p, a mitochondrial phosphoprotein involved in signaling cell-wall stress to the PKC1-MPK1 cell integrity pathway [38,39], was found to decrease upon AA-PCD induction.

3.3.7. Translation machinery

Elongation factor Eft2p was found as protein fragments in both strains and its amount was down-regulated upon AA-PCD induction. 40S and 60S ribosomal subunits, Rpl12ap and Rpl8bp, were altered. Rpl12ap was up-regulated in either samples, whereas Rpl8bp was up-regulated in WT cells and down-regulated in *Δyca1* cells.

3.3.8. Other processes

Hmf1p, a member of the highly conserved p14.5 protein family was found to be down-regulated both in WT and in *Δyca1* cells undergoing AA-PCD. *HMF1* has a paralog, *MMF1* (mitochondrial matrix factor 1) that arose from the whole genome duplication. Mmf1p is involved in maintenance of mitochondrial genome [40], it is required for transamination of isoleucine but not of valine or leucine and may regulate specificity of branched-chain transaminases Bat1p and Bat2p [41] (see above).

3.4. Proteins and metabolites found altered only in WT AA-PCD cells

Proteins altered only in WT AA-PCD cells are described below and grouped on the basis of their functions.

3.4.1. Carbohydrate metabolism

The amount of the glycolytic enzyme triose phosphate isomerase (Tpi1p) was found to decrease only in WT cells, while in *Δyca1* cells it did not show a statistically significant difference. Accordingly, a decrease in glycolytic intermediates was detected in both AA-PCD strains (see above). Yet, both PPP intermediates ribose-5-phosphate and sedoheptulose-7-phosphate showed a significantly higher fold-increase in WT AA-PCD cells than in *Δyca1* cells (Fig. 4) in accordance with PPP stimulation induced by Tpi1p inhibition [42].

3.4.2. Amino acid metabolism

Ketol-acid reductoisomerase (Ilv5p) and S-adenosylmethionine synthase 1 (Sam1) showed decreased expression. Ilv5p is involved in branched-chain amino acid biosynthetic process, as well as in mitochondrial genome maintenance. Sam1p catalyzes transfer of the adenosyl group of ATP to the sulfur atom of methionine to form S-adenosyl-L-methionine (AdoMet), a major constituent of intermediary metabolism. AdoMet is a cofactor involved in methylation of organic molecules, polyamine and biotin synthesis, as well in the synthesis of queuine, a modified base of tRNAs of prokaryotes and eukaryotes [43]. However, metabolomic analysis of amino acid content of AA-PCD WT *versus* control cells revealed higher levels of leucine, isoleucine, valine, tryptophane, methionine, threonine, phenylalanine and homoserine.

3.4.3. Nucleotide metabolism

Ura5p and Fur1p, involved in pyrimidine biosynthesis and salvage pathways, were down-regulated in wild type AA-PCD. Also, Adk1, required for purine metabolism, is also found to have decreased expression

Table 2
Differentially expressed proteins in Δyca1 AA-PCD.

Proteins identified	Biological protein function	NCBI accession number	Theoretical Mr (Da)	Theoretical pI	Spot number	No of peptides identified	Mascot score	Fold change	Expression level
Carbohydrate metabolism									
Eno1	Enolase I (phosphopyruvate hydratase)	gi|171455	46,830	6.16	1468	5	232	2.4	Down
Eno2	Enolase II	gi|6321968	46,942	5.67	899 (fragment)	7	276	2.2	Down
					528	19	957	3.1	Down
					525	7	497	2.5	Down
					526	13	740	3.2	Down
Tdh3	Glyceraldehyde-3-phosphate dehydrogenase, isozyme 3	gi|45269553	35,780	6.72	1421	10	437	2.0	Down
					720 (fragment)	11	638	2.9	Down
					666	16	683	2.4	Down
					661	12	594	2.1	Down
					1006	5	335	3.0	Down
Hxk2	Hexokinase isoenzyme 2	gi|3710	27525	5.19	1019	5	261	3.6	Down
Pgi1	Phosphoglucose isomerase (Glucose-6-phosphate isomerase)	gi|6319673	61,261	6.00	169	5	231	3.4	Up
Adh2	Alcohol dehydrogenase II	gi|171029	37,162	6.31	1252	2	114	2.7	Down
Adh1	Alcohol dehydrogenase I	gi|223142	31,954	6.38	520	9	492	2.3	Down
					514	10	419	2.3	Down
Fba1	Fructose 1,6-bisphosphate aldolase	gi|6322790	39,881	5.51	644	6	199	2.5	Down
Pdc1	Pyruvate decarboxylase	gi|256270485	46,909	5.74	1638 (fragment)	6	264	2.6	Down
		gi|6323073	61,685	5.80	45	7	250	2.3	Up
Pgk1	Phosphoglycerate kinase	gi|10383781	44,768	7.11	1771	14	667	2.3	Down
Amino acid metabolism									
Bat1	Mitochondrial branched-chain amino acid (BCAA) aminotransferase	gi|151944153	43,798	8.80	1652	2	97	2.0	Up
Cys3	Cystathionine gamma-lyase	gi|6319307	42,516	6.06	706 (fragment)	3	210	3.3	Down
Nucleic acid metabolism									
Ado1	Adenosine kinase	gi|365764754	36,501	4.99	1711	10	476	2.3	Down
Transcription/translation machinery									
Eft2	Elongation factor 2 (EF-2)	gi|6320593	93,686	5.92	609 (fragment)	6	352	2.0	Down
Hef3	Translational elongation factor EF-3	gi|173214	116,775	5.73	1444 (fragment)	2	97	2.1	Down
Tif6	Translation initiation factor 6	gi|6325273	26,669	4.54	553	2	105	2.0	Down
Rpl1a	Ribosomal 60S subunit protein L1A	gi|6325036	24,189	9.72	1730	4	130	3.4	Up
Rpl7a	Ribosomal 60S subunit protein L7A	gi|6321362	27,621	10.15	1730	5	185	3.4	Up
Rpl12a	Ribosomal 60S subunit protein L12A	gi|6320781	17,869	9.43	1697	12	581	3.1	Down
Rpl8b	Ribosomal 60S subunit protein L8B	gi|6322984	28,151	10.02	1141	4	178	2.0	Up
Rpl13b	Ribosomal 60S subunit protein L13B (YMR142Cp-like protein)	gi|207342264	22,511	11.08	1730	6	318	3.4	Up
Rpl22a	Ribosomal 60S subunit protein L22A	gi|6323090	13,685	5.91	1786	1	61	2.0	Down
Rps0a	Ribosomal 40S subunit protein S0A	gi|6321653	28,064	4.65	1754	2	60	2.6	Down
Ssz1	Hsp70 protein that interacts with Zuo1p	gi|37362658	58,316	4.94	1662 (fragment)	4	136	2.9	Down
Ses1	Seryl-tRNA synthetase	gi|6320226	53,732	5.80	169	5	179	3.4	Up
Protein folding/turnover/transport									
Cct2	Chaperonin containing TCP-1 subunit beta of the cytosolic chaperonin Cct ring complex	gi|6322049	57,510	5.80	169	7	394	3.4	Up
Pam16	Presequence translocase-associated motor	gi|6322357	16,263	9.43	1697	5	229	3.1	Down
Sar1	Secretion-associated, Ras-related GTP-binding protein of the ARF family	gi|6325038	21,494	5.21	1444	3	114	2.1	Down
Smt3	Suppressor of Mif two ubiquitin-like protein of the SUMO family	gi|6320718	11,590	4.92	1667	2	114	2.1	Down
Stress response									
Ssa1	Stress-Seventy subfamily A Hsp70 family ATPase	gi|6323371	33,696	4.75	1662	4	168	2.9	Down
Ssa2	Stress-Seventy subfamily A	gi|6323004	69,599	4.95	540 (fragment)	8	416	2.0	Down
					1261 (fragment)	7	285	2.3	Up
		gi|151941146	69,772	5.00	645 (fragment)	13	760	2.8	Down
		gi|151941387	69,772	5.00	643 (fragment)	12	741	2.6	Down
Ssb1	Stress-Seventy subfamily B Hsp70 family ATPase	gi|6319972	66,732	5.32	1706	22	967	2.0	Up
					723 (fragment)	9	460	2.7	Down
Ssb2	Stress-Seventy subfamily B Hsp70 family ATPase SSB2	gi|151944335	66,669	5.32	120	34	2015	3.4	Up
Sse1	ATPase component of the heat shock protein Hsp90 chaperone complex	gi|533365	77,647	5.12	400 (fragment)	4	260	2.9	Down
Zeo1	Zeocin resistance protein	gi|6324463	12,582	5.43	809	3	127	2.2	Down
Ahp1	Alkyl hydroperoxide reductase	gi|6323138	19,274	5.01	987	5	292	3.4	Down
					984	6	329	4.0	Down
Tsa1	Thioredoxin peroxidase	gi|6323613	21,690	5.03	984	3	95	4.0	Down
Hsp82	Hsp90 chaperone	gi|2624655	24,831	4.86	823	3	109	2.3	Down
Sba1	Increased sensitivity to benzoquinone ansamycins	gi|6322732	24,123	4.46	1754	2	77	2.6	Down

Table 2 (*continued*)

Proteins identified	Biological protein function	NCBI accession number	Theoretical Mr (Da)	Theoretical pI	Spot number	No of peptides identified	Mascot score	Fold change	Expression level
Sis1	Type II HSP40 co-chaperone that interacts with the HSP70 protein Ssa1p	gi|6324321|	37,567	9.02	427	1	33	3.6	Up
Fatty acid biosynthesis									
Fas2	Alpha subunit of fatty acid synthetase	gi|2326840	34,921	6.12	1533	2	82	2.3	Down
Cell signaling									
Bmh1	Brain modulosignalin homologue 14-3-3 protein, major isoform	gi|671634	30,272	4.87	1765	14	681	2.7	Down
Asc1 (Chain A)	G-protein beta subunit; core component of the small (40S) ribosomal subunit	gi|223674073	34,757	5.64	489	11	653	2.2	Down
Others									
Vma1	Vacuolar membrane Atp-ase	gi|3417405	68,023	5.17	1706	15	691	2.0	Up
Unknown									
Hmf1	Homologous Mmf1p Factor	gi|398364461	14,011	5.28	1638	1	105	2.6	Down
Unidentified proteins									
1035									Down

in WT apoptotic cells. Thus, overall down-regulation of major enzymes of nucleotide metabolism indicates that both *de novo* biosynthesis as well as nucleotide salvage pathways are compromised in WT cells following AA-treatment.

3.4.4. Protein folding/degradation

The expression of Ubc4p, ubiquitin-conjugating enzyme that mediates selective degradation of short-lived and abnormal proteins, was found to be up regulated upon AA-treatment. The expression of Egd2p, alpha subunit of the heteromeric nascent polypeptide-associated complex (NAC) was found to decrease in WT cells *en route* to AA-PCD.

3.4.5. Stress response

High-Copy Hsp90 suppressor (Hch1p) was down-regulated, like the majority of other stress response proteins.

3.4.6. Translation machinery

Different elongation factors were found to be down-regulated, whereas 40S and 60S ribosomal subunits were found to be up-regulated *en route* to AA-PCD. Translation elongation factors Tef1p and Yef3p were found as protein fragments.

3.4.7. Cytoskeletal proteins

Actin, a structural protein involved in cell polarization, endocytosis and other cytoskeletal functions, was found to be down-regulated *en route* to AA-PCD in WT cells. Actin is shown to be involved in yeast cell stress response and the control of signaling through the RAS/cAMP/PKA pathway, pheromone and cell wall integrity MAPK pathways and TOR pathways [44]. The corruption of actin leads to the induction of apoptosis *via* the hyperactivation of RAS signaling. This combination leads us to suggest that actin-mediated apoptosis serves as a mechanism by which yeast cells that are unable to respond to a number of stresses can be removed from a population. Furthermore, alpha-tubulin (Tub1p), which polymerizes into microtubules with beta-tubulin, was found to be down-regulated in WT cells undergoing AA-PCD. Microtubules are conserved cytoskeletal elements known to be involved in chromosome segregation during mitosis and meiosis, spindle orientation and nuclear migration during mitosis and mating.

3.5. Proteins and metabolites found altered only in Δyca1 AA-PCD cells

Proteins and related metabolites differentially expressed exclusively in *Δyca1* AA-PCD cells (Fig. 3 set C) were grouped on the basis of their functions as follows.

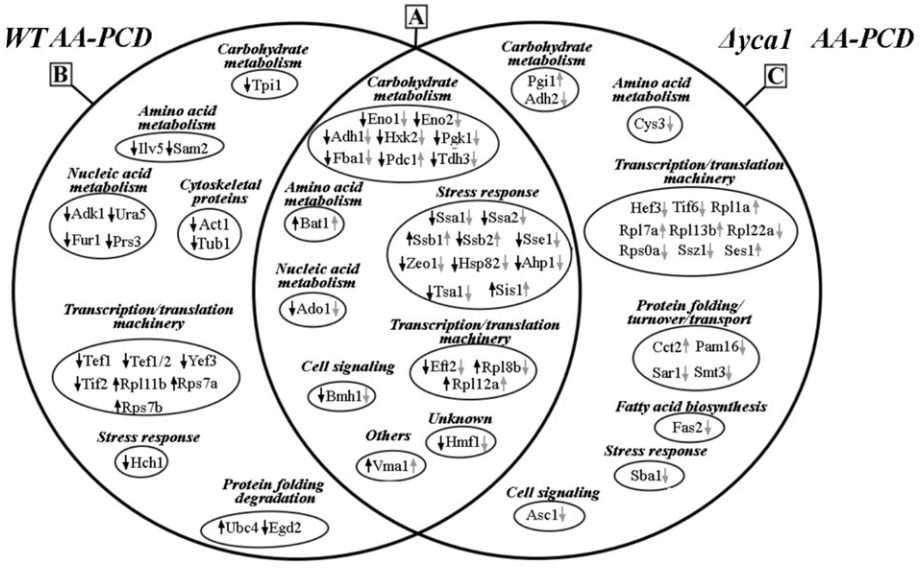

Fig. 3. Venn diagram representing the proteins differentially expressed after 150 min AA-PCD both in WT and *Δyca1* cells (A); exclusively in WT cells (B, WT AA-PCD); exclusively in *Δyca1* cells (C, Δyca1 AA-PCD); the black and gray arrows represent the proteins down- or up-regulated in WT or in *Δyca1* cells, respectively.

3.5.1. Carbohydrate metabolism

Alcohol dehydrogenase II (Adh2p), an enzyme that catalyzes the reverse reaction of ethanol conversion to acetaldehyde was down-regulated. Phosphoglucose isomerase (Pgi1p), together with Pdc1p, were the only glycolytic enzymes increased in *Δyca1* apoptosis. Thus, there is a strong down-regulation of glycolytic enzymes in *Δyca1* cells *en route* to AA-PCD, but the fold-change of protein abundance was smaller than WT cells. In fact, in general, glycolytic intermediates were less decreased, while those of PPP fewer increased in *YCA1*-knock-out AA-PCD (Fig. 4) respect in wild type AA-PCD.

3.5.2. Amino acid metabolism

Cys3p expression (detected only as a protein fragment) was decreased upon AA-PCD. Cystathionine gamma-lyase (Cys3p) catalyzes one of the two reactions involved in trans-sulfuration pathway that yields cysteine from homocysteine, as well as a reaction in threonine degradation pathway that yields cystathionine. Differently from WT AA-PCD cells, metabolome analysis showed that general amino acid content decreased in *Δyca1* cells *en route* to AA-PCD.

3.5.3. Protein folding/degradation/transport

A subunit of cytosolic chaperonin Cct ring complex, Cct2p, was found to be up-regulated upon AA-PCD. These chaperones assist the folding of proteins upon ATP hydrolysis and are known to play a role, *in vitro*, in the actin and tubulin folding, and may play a role in mitotic spindle formation. Smt3p protein involved in protein SUMOylation is found to be down-regulated in *Δyca1* AA-PCD. Two other proteins, Pam16p and Sar1p, involved in intracellular protein transport, are also found to be down-regulated. Pam16p is the constituent of the import motor (PAM complex) component of the Translocase of the Inner Mitochondrial membrane (TIM23 complex) involved in protein import into mitochondrial matrix. Sar1p is Secretion-Associated, Ras-related GTP-binding protein of the ARF family involved in coat protein complex II (COPII) vesicles — mediated transport of proteins from the endoplasmic reticulum (ER) to the Golgi. Sar1p is a COPII vesicle core component involved in the regulation of COPII vesicle coating [45].

3.5.4. Cell signaling

Asc1p was also found to be down-regulated *en route* to AA-PCD. Asc1p is yeast ortholog of RACK1 (receptor for activated protein kinase C1) that

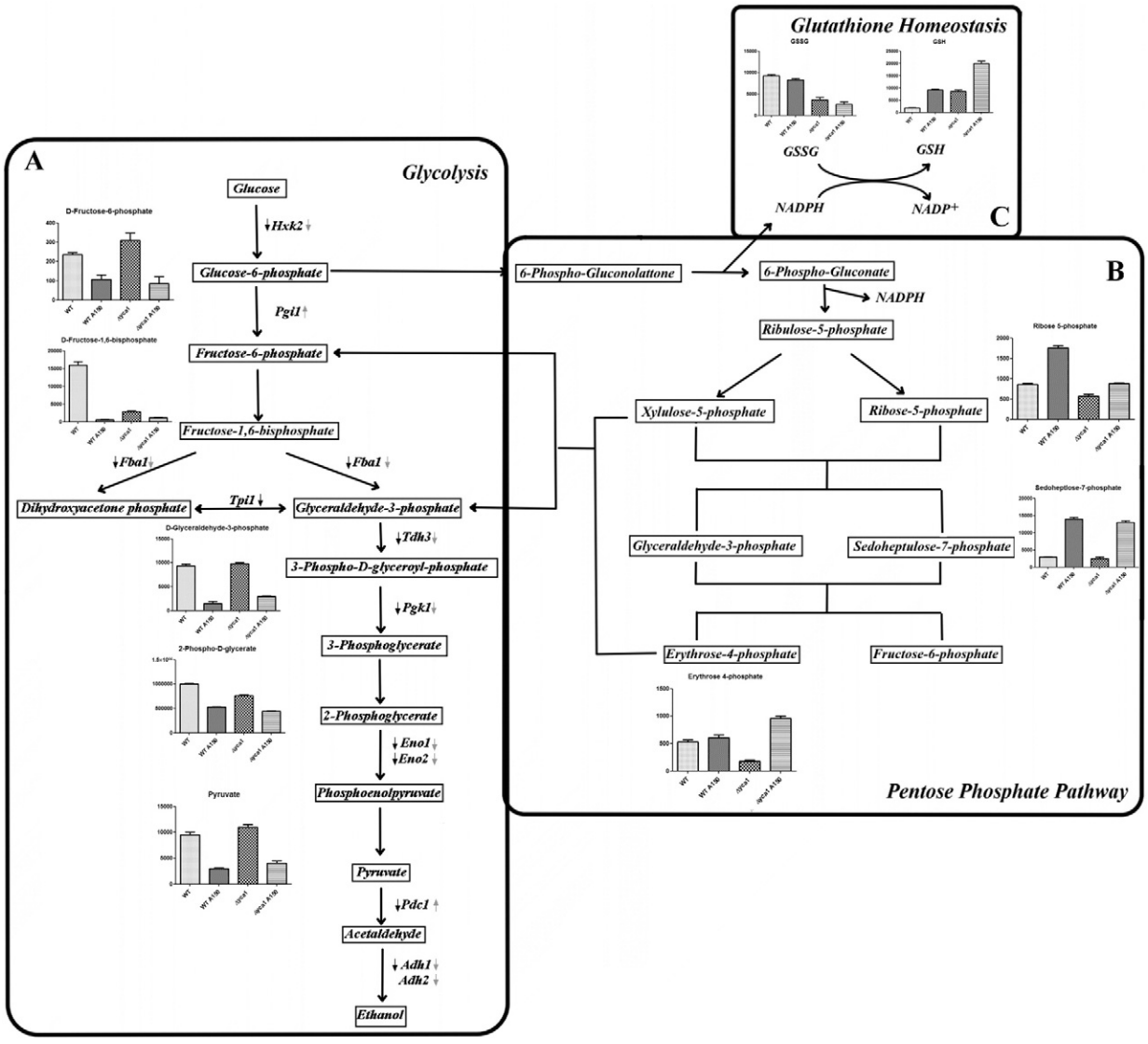

Fig. 4. Absolute metabolomic quantification (arbitrary ion counts) of metabolites from carbohydrate metabolism (panel A) (glycolysis), pentose phosphate pathway (panel B), glutathione homeostasis (panel C), in WT or *Δyca1* W303-1B yeast cells before and after (A150) 150 min AA-PCD. Data are presented as mean ± SD.

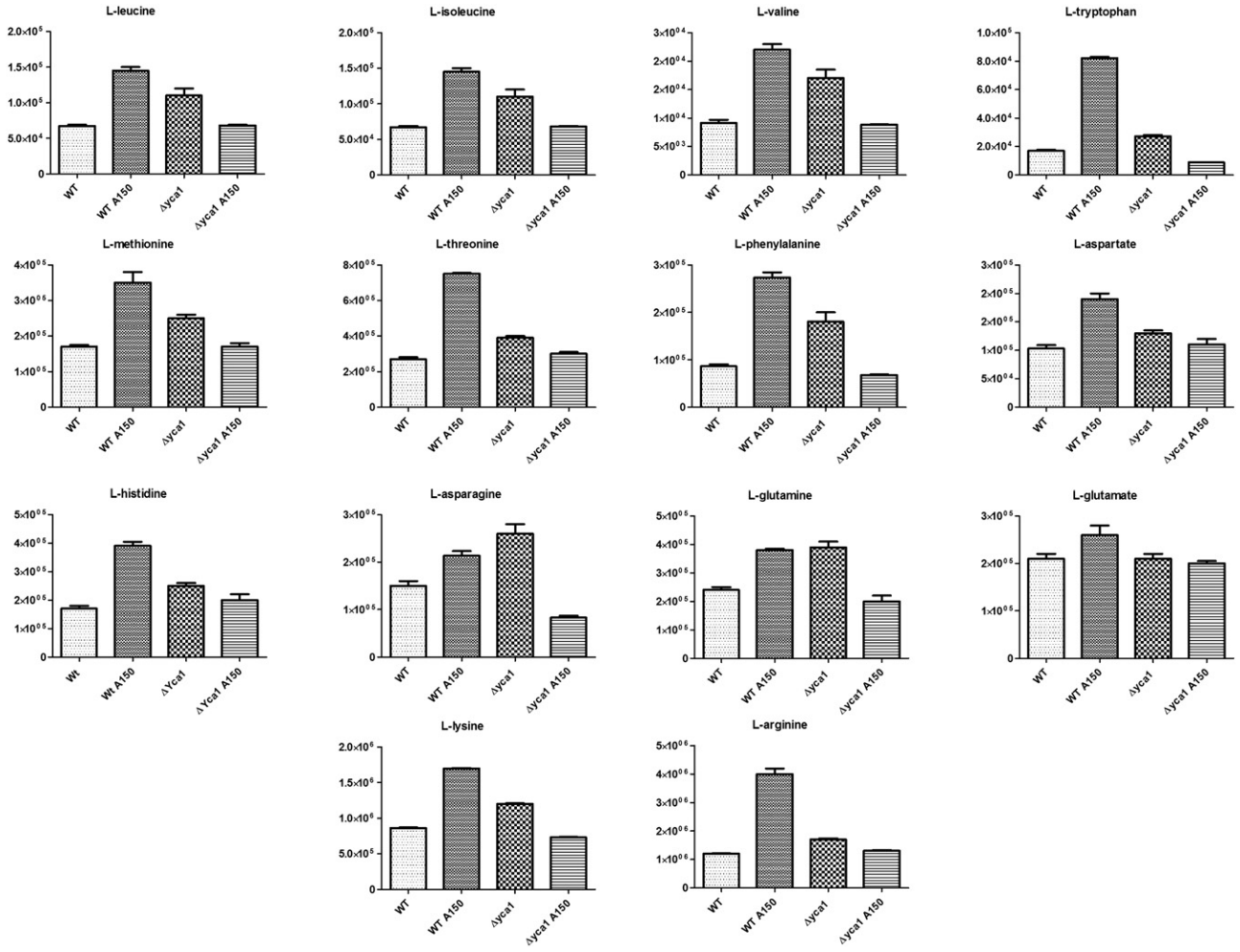

Fig. 5. Absolute metabolomic quantification (arbitrary ion counts) of amino acids in WT and *YCA1*-knock out W303-1B cells before and after (A150) 150 min AA-PCD. Data are presented as mean ± SD.

has an inhibitory effect on glucose signaling and cAMP production [46]. As a core conserved ribosomal protein, Asc1p also has a role in transcriptional repression [47].

3.5.5. Stress response

Sba1p was found to be down expressed, such as the other proteins with the same function. Sba1p is a co-chaperone that binds and regulates Hsp90 family chaperons; it is homologous to human p23 proteins, responsible for the reconstitution of human telomerase activity *in vitro*.

3.5.6. Translation machinery

It is interesting to note that the proteins involved in cytoplasmic transcription and translation and ribosomal biogenesis are quantitatively the biggest group of proteins affected by AA-PCD in *Δyca1* cells and that 9 out of the total 12 proteins (75%) affected, were identified only in *Δyca1* cells. Out of 12 proteins affected, 5 were up- and 7 down-regulated. Structural constituents of ribosome, Rpl1ap, Rpl7ap, Rpl8bp, Rpl13bp, involved in cytoplasmic translation, were found to be up-regulated, whereas Rpl12ap, Rpl22ap, Rps0ap and Ssz1p (a fragment) were down-regulated. Ses1p, seryl-tRNA synthetase, was found to be up-regulated, whereas Ssz1p, also involved in cytoplasmic translation, was found to be down-regulated. Translation initiation factor 6 (TIF6) was found to be down-regulated, as well as translational elongation factor EF-3 (HEF3) and elongation factor 2 (EF-2). Hef3p and Eft2p were identified as protein fragments.

3.5.7. Fatty acid biosynthesis

Exclusively in *Δyca1* AA-PCD cells the expression of alpha subunit of fatty acid synthetase (Fas2p) was found to decrease while it remained unaffected in WT cells. Fas2p catalyzes the formation of long-chain saturated fatty acids from acetyl-CoA, malonyl-CoA and NADPH. In *S. cerevisiae* fatty acid biosynthesis, only the acetyl-CoA carboxylase activity (Acc1p) is separate, all other activities are distributed between two proteins, Fas1p and Fas2p, the beta and alpha subunits of a large, barrel-shaped complex containing 6 copies of each protein [48,49]. Together, the six Fas1p and six Fas2p subunits form six independent reaction centers, each containing all enzyme activities required for synthesizing long chain fatty acids from acetyl- and malonyl-CoA [50,51]. *FAS2* encodes the acyl-carrier protein domain and three independent enzymatic functions: 3-ketoreductase, 3-ketosynthase and phosphopantetheinyl transferase. Because malonyl coenzyme A (malonyl-CoA) provides the 2-carbon unit for *de novo* long-chain fatty acid synthesis by FAS [52], we analyzed *Δyca1* cells before and after 150 min AA-PCD for malonyl CoA content. We observed accumulation of malonyl CoA in AA-PCD *Δyca1* cells (Fig. 6A) supporting the decrease of fatty acid synthesis. Since long-chain fatty acids are precursors of sphingolipids (Fig. 6 B) which also play an important role as signaling molecules in the regulation of PCD [53], a lipidomic analysis was performed in *Δyca1* control and AA-PCD *Δyca1* cells. The results revealed that several sphingolipid species increased in *Δyca1* cells undergoing AA-PCD (Fig. 6C). We observed a decrease in the level of dihydrosphingosine-1-phosphate (DHS-1-P), phytosphigosine (PHS)

and phytosphingosine-1-phosphate (DHS-1-P). The level of most phytoceramide and dihydroceramide species increased in *Δyca1* AA-PCD cells (Fig. 6C).

In agreement with our results, Rego and co-workers have already suggested that ceramide production contributes to AA-PCD, providing indication that ceramide metabolism is involved in cyt c release and mitochondrial fragmentation [54]. Since it has already been shown that, in distinction from WT cells, AA-PCD occurs without cyt c release in *Δyca1* cells [15], we analyzed mitochondrial morphology either in WT or *Δyca1* cells before or after AA-PCD in order to gain insights into the role of *YCA1* in ceramide-dependent mitochondrial damage. To this aim both strains were transformed with a plasmid containing a DNA sequence coding for a mitochondrial pre-sequence fused to the GFP coding region under the control of the strong constitutive ADH promoter [25]. The yeast strains obtained, named WT-mtGFP and *Δyca1*-mtGFP, were grown in YPD medium up to exponential phase and analyzed by confocal microscopy (Fig. 7). A green fluorescence of the characteristic branched tubular mitochondrial network was observed in either cell types. AA-PCD was induced in either WT-mtGFP or *Δyca1*-mtGFP and cells were observed by confocal microscopy after 75 and 150 min. In both cases AA-PCD occurrence was confirmed at 150 min by clonogenic assay (10 and 30% viability for WT-mtGFP or *Δyca1*-mtGFP, respectively) and DNA fragmentation analysis (about 50% TUNEL-positive cells for either yeast strains). *Δyca1*-mtGFP cells showed a punctuated mitochondrial morphology at both times analyzed, indicative of mitochondrial damage [55]. Similarly WT-mtGFP showed mitochondrial fragmentation as already reported [56,57]. Our results shows that, notwithstanding the lack of cyt c release in *Δyca1* cell AA-PCD [16], mitochondrial fission occurs *en route* to both WT and *Δyca1* cell AA-PCD pathways.

4. Discussion

Yeast has been successfully used as a model system to elucidate several aspects of apoptosis regulation in mammalian cells, particularly of the intrinsic mitochondrial pathway [2,7,53,58–60]. One of the major functions of mitochondria in mammalian apoptosis is the release of cyt c to activate the caspase cascade through apoptosome formation [61]. With this respect yeast metacaspase-encoding gene *YCA1* has been shown to be a positive regulator of yeast PCD induced by different stimuli [62], including acetic acid [13]. Yet, no apoptosome has been shown in yeast and a variety of proteases have been shown to participate in yeast PCD, not all of these activities being associated with *YCA1* [6]. Importantly, we have previously shown and here confirmed that AA-PCD occurs both in WT and *Δyca1* cells but with a lower death rate in the latter cells. In addition it has been shown that *Δyca1* cell AA-PCD occurs without cyt *c* release [14].

Comparison of the combined proteomics and metabolomic profiling of AA-PCD WT or *Δyca1* cells performed in this study clearly confirmed that the presence or absence of *YCA1* does not affect the cell fate as highlighted in Fig. 3 set A which reports the proteins differentially expressed in both WT and *Δyca1* cells. Two classes of proteins and related metabolites were shown to be most affected during AA-PCD process independently of *YCA1*: those involved in carbohydrate metabolism and in stress response. Importantly our study showed that *YCA1* can modulate the AA-PCD mechanism by regulating glycolytic metabolism and PPP as well as ceramide metabolism. Here we discuss separately the proteins and related metabolisms found to be differentially expressed in both WT and *Δyca1* cells or specifically in one of each strain undergoing AA-PCD (see Fig. 3) thus allowing identification of the molecules and cellular processes regulated by *YCA1 en route* to PCD.

4.1. Yeast proteins and metabolisms altered en route to AA-PCD independently of the presence of YCA1

Two classes of molecules appeared to be most affected by PCD-triggering acetic acid treatment as also revealed by metabolome analysis: those involved in carbohydrate metabolism and in stress response. A general decrease in the levels of enzymes involved in glycolysis, fermentation and other metabolic functions were observed (Fig. 3A). The decrease of glycolytic rate can be correlated to growth arrest to save energy necessary for PCD occurrence, as already reported in another yeast strain [23]. Moreover, metabolomic analysis showed a diversion from the main glycolytic pathway towards the PPP in both WT and knock-out strain. This shift may result in accumulation of NADPH, an essential coenzyme for glutathione disulfide (GSSG) reconversion to glutathione (GSH) which is considered a natural self-defensive mechanism of cells to cope with oxidative stress since GSH plays an essential role in maintaining the intracellular redox environment [63,64]. Accordingly, we found GSH accumulated in either cell types after 150 min AA-PCD. It should be noted that the remarkable high content of GSH found in *Δyca1* AA-PCD cells indicates an intrinsic anti-oxidant capacity of *YCA1*-lacking cells in agreement with the fact that *Δyca1* cell AA-PCD pathway is insensitive to antioxidant N-acetyl cysteine [15].

In addition, we noted a dramatically decrease of stress response proteins. Like in [23], numerous members of Hsp70 family showed a reduced intensity upon acetic acid-induced apoptosis. It is known that in mammalian cells chaperones present anti-apoptotic activity, by preventing caspase activation or by neutralizing the apoptosis-inducing factor (AIF) function through direct interaction [65]. This suggests that acetic acid-induced PCD can be enhanced by the absence of this anti-apoptotic action. A down regulation of Bmh1, a homologue of human 14-3-3 proteins, occurs. This protein is known for its capacity to protect cells against stress-induced apoptosis [36]. Thus, the minor abundance of this protein reflects the apoptotic state of cells that underwent AA-treatment.

Vacuolar acidity was found to modulate mitochondrial function and yeast life span [45]. Prevention of decline of vacuolar acidity, which occurs during replicative aging, was found to suppress mitochondrial dysfunction and extend lifespan in yeast. Furthermore, vacuolar protease Pep4p, was found to be involved in mitochondrial degradation and is released into the cytosol upon AA-treatment [57]. Finally, Ca^{2+}-sensitive Pet^{-} mutants have been reported to have mutations in the family of *VMA* genes, including *VMA1*, which affected Ca^{2+} homeostasis, glycerol metabolism and phospholipid metabolism in these cells [66]. All of these Pet^{-} mutants have lost vacuolar membrane H^{+}-ATP-ase activity, vacuolar Ca^{2+} uptake activity and the ability to acidify the vacuole *in vivo*.

4.2. Yeast proteins and metabolisms altered en route to AA-PCD in WT cells

An important glycolytic enzyme, triose phosphate isomerase (Tpi1p) decreases during AA-PCD only in wild type cells (Fig. 3B). Tpi1p is known to be a potent inhibitor of PPP, in fact Ralser and co-workers [67] have demonstrated that reduced activity of Tpi causes a re-configuration of central metabolism, leading to increased flux of the PPP and increased stress resistance in yeast. This evidence is in agreement with our observation that certain PPP intermediates showed a higher fold-change in WT cells than in *YCA1*-knock-out cells during AA-PCD.

Except for Ado1p, which we have already seen that was altered in both PCD pathways, the proteins involved in nucleic acid metabolism were dramatically down regulated only in wild type cells. This aspect can induce to think that Yca1p influences strongly this metabolism. In fact Adk1p which catalyzes phosphate group transfer from ATP to AMP, Ura5p which represents the fifth enzyme in *de novo* biosynthesis of pyrimidines, Fur1p involved in UMP synthesis and Prs3p which synthesizes phosphoribosylpyrophosphate, were all down-regulated. The decreased glucose metabolism *en route* to AA-PCD leads to decreased ATP generation as well as loss in generation of many biosynthetic precursor molecules, including nucleotides [68]. All energy available in the cell is used in order for PCD to occur, consequently all biosynthetic pathways appear to be down regulated. Accordingly, the translation

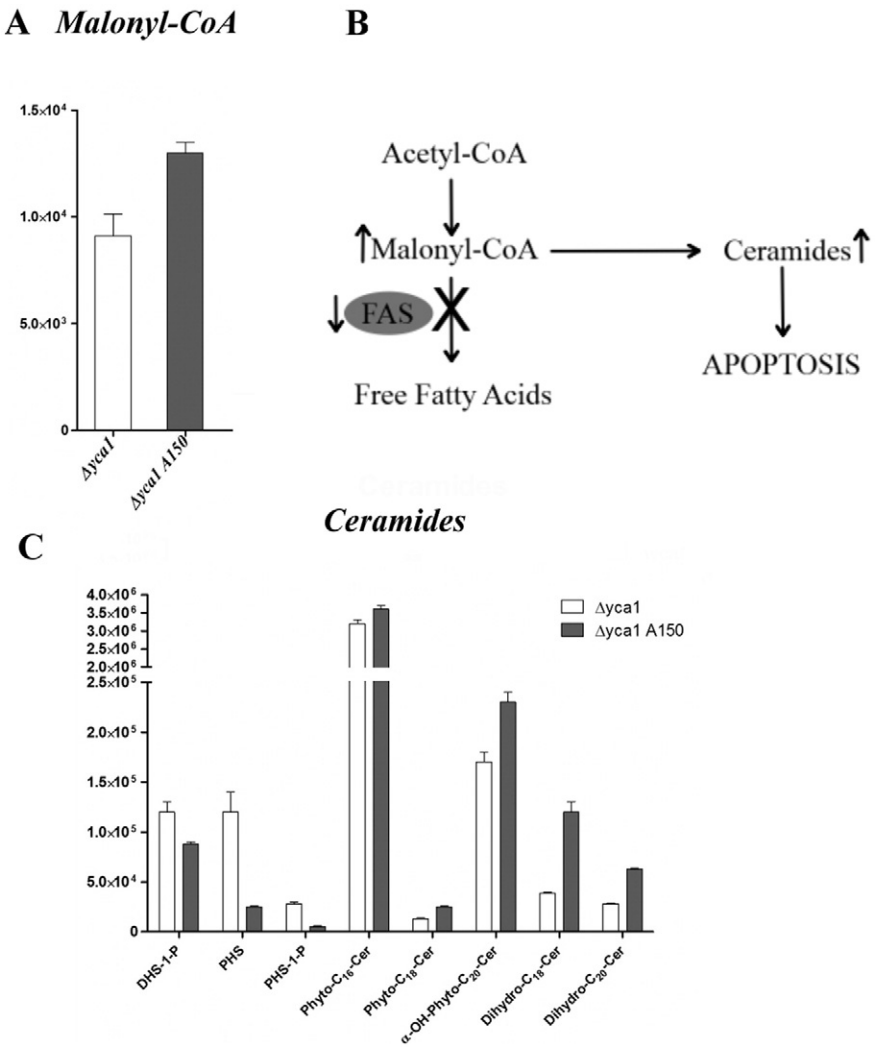

Fig. 6. Absolute metabolomic quantification (arbitrary ion counts) of malonyl CoA (panel A), ceramides (panel C) in cells lacking *YCA1* gene in the presence and absence of acetic acid. Schematic metabolism involving malonyl CoA, FAS2 and ceramides (panel B).

machinery slowed down. Cells do not misspend energy for biosynthesis of new proteins, rather seek to obtain from their degradation. In fact, in WT cells, Ubc4p, the ubiquitin-conjugating enzyme (E2) was accumulated *en route* to AA-PCD. Ubc4p, as well as Ubc1p and Ubc5p, was found to mediate selective degradation of short-lived and abnormal proteins [69]. Ubc4p generates high molecular weight ubiquitin–protein conjugates and comprise a major ubiquitin-conjugation activity in yeast cells. Moreover, this enzyme is a central component of the cellular stress response. Furthermore, Chuang and co-workers [70] have demonstrated that Ubc4p has a specific role in degradation of co-translationally damaged proteins and this can be explained by the failure of the translation machinery. The abundance of Ubc4p is correlated with the increase of proteasome activity that is needed for AA-PCD to occur [71]. In fact, unlike certain mammalian and plant cells in which proteasome inhibition was found during PCD, in yeast there is a transient increase in proteasome activity from 60 up to 150 min after AA-induction because of increased efficiency of catalytic activity [71]. In support of this, Egd2p, the alpha subunit of the nascent polypeptide-associated complex, which appears to be less abundant, is known to be degraded *via* the proteasome pathway in stress condition. In addition, protein degradation by the ubiquitin–proteasome pathway, determine accumulation of amino acids, as reported by Lecker [72], as observed in WT AA-PCD cells in this study. The rapid degradation of specific protein permits adaptation to new physiologic condition.

4.3. Yeast proteins and metabolisms altered en route to AA-PCD in Δyca1 cells

We show here that AA-PCD occurs with a decline in the glycolytic pathway and increase in PPP, although at a lower level in *Δyca1* than in WT cells; translation of new proteins was blocked, stress response proteins were down regulated allowing PCD to proceed (Fig. 3C). Importantly, given the decrease in the expression of Fas2p protein involved in fatty acid synthesis, together with both the increase of malonyl-CoA and ceramides and decrease in long chain base phosphates, our data strongly suggest the existence of an alternative *YCA1*-independent AA-PCD pathway mediated by ceramides (Fig. 6B).

In yeast, like in mammalian cells, ceramide levels increase in response to diverse stress treatment [73,74] and the formation of ceramide channels has been proposed as another mechanism mediating the release of pro-apoptotic proteins from mitochondria during the apoptosis [53,75,76]. Therefore, several sphingolipid species control mitochondrial PCD pathway in yeast as well as in mammals [53]. Mitochondrial fission was shown here to occur both *en route* to *YCA1*-dependent and *YCA1*-independent AA-PCD pathways (Fig. 7) without cyt c release in the latter case [15]. Our results strongly suggest that ceramides have an active role in cyt c release in yeast AA-PCD, possibly through the formation of ceramide pore as already suggested by Rego et al. [54]. Whether the lack in cyt c release observed in *Δyca1* AA-PCD

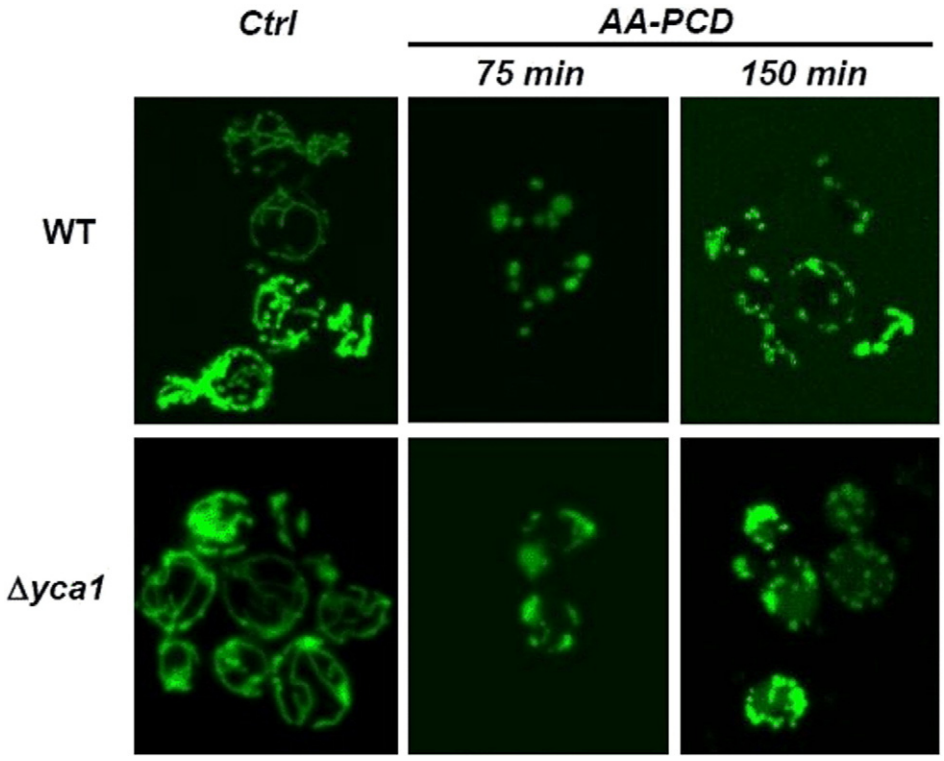

Fig. 7. Mitochondrial fission occurs *en route* to WT and *Δyca1* cell AA-PCD. Either WT-mtGFP or *Δyca1*-mtGFP cells were grown up to early-exponential phase and treated with 80 mM acetic acid. Cells were observed by confocal laser scanning microscopy before (Ctrl) and after 75 and 150 min AA-PCD. Representative z-stack images are reported.

is related to changes in the mitochondrial level of ceramides and with their ability to form ceramide pores needs further investigation.

In fairly good agreement with our results, it has been shown that an externally added analogue of ceramide can induce yeast PCD through a ROS-dependent mechanism, which is not dependent on yeast metacaspase gene *YCA1* [77]. This study suggests an important and novel *FAS2*-dependent relation between sphingolipid metabolism and yeast metacaspase gene in PCD progression.

Although transient proteasome activation is needed for AA-PCD to occur [71], we noted in *Δyca1* cell AA-PCD a general decrease of some proteins involved in protein folding degradation as also revealed by reduced degradation of proteins and amino acid depletion.

Decreased abundance of Smt3p, an ubiquitin-like protein of the SUMO family, and also of Sar1p, a GTP-binding protein involved in transport vesicle formation during ER to Golgi protein transport and related to proteolytic process, suggests that the absence of *YCA1* affects the proteolysis. It has been shown that proteasome levels and the proteolytic capacity of cells are unaffected in *YCA1*-knock-out cells [19]. Thus, it is tempting to speculate that *YCA1* is involved in regulation of ubiquitination pathways. In fact, H_2O_2-mediated stress leads to up-regulation of the 20S proteasome, but suppression of ubiquitination activities [19].

5. Conclusion

Recent advances in various 'omics' technologies enable quantitative monitoring of the abundance of various biological molecules in a high-throughput manner, and thus allow determination of their variations between different biological states. In this study the integration of proteomics and metabolomics, has proved a potent tool of investigation on AA-PCD mechanisms dependent or independent on *YCA1* and it will prove pivotal for understanding how the individual components in the system interact and influence overall cell metabolism and ultimately its fate.

Although a common decrease in glycolytic cycle enzymes and shift towards the PPP happened in both cases, those biochemical features are predominant in WT cell AA-PCD pathway allowing us to conclude that metacaspase function could play a key role in the shift from glycolysis to PPP during PCD. Furthermore, this study emphasized the central role of metacaspase gene in proteolysis *en route* to AA-PCD, because its presence or absence affects the ubiquitin–proteasome system through the modulation of crucial regulatory proteins.

Finally, we provided first experimental evidence of a mechanism which suppresses ceramide-mediated PCD through *YCA1*-dependent FAS2 regulation, confirming that activation of phyto-C-16, phyto-C-18, α-OH-phyto-C20, dihydro-C-18 and dihydro-C-20 ceramides can trigger PCD in yeast [54]. Ceramides are bioactive sphingolipids that mediate antiproliferative and pro-apoptotic signaling in response to various stress stimuli [78]. The inhibition of Fas2 elicits cell cycle arrest and apoptosis, so it is considered a potential drug target for oncology [79]. A model for the apoptotic pathway induced by FAS inhibition, whereby inhibition of FAS leads to accumulation of malonyl-CoA, which in turn inhibits carnitine palmitoyltransferase I, resulting in up-regulation of ceramide followed by induction of the proapoptotic genes BNIP3, TRAIL, and DAPK2, has been proposed [80]. The results of this study expand the use of yeast as a model to study PCD pathways in normal and cancer-related conditions [81,82].

Supplementary data to this article can be found online at http://dx.doi.org/10.1016/j.jprot.2015.08.003.

Conflict of interest

Disclose any conflicts of interest.

Acknowledgements

This work has been funded by grants from project FIRB-MERIT RBNE08HWLZ, the Italian Ministry of Economy and Finance to the

CNR for the Project "FaReBio di Qualità" and project BioNet –PTP - PO Regione Puglia FESR 2000-2006 to S.G.

References

[1] D. Carmona-Gutierrez, T. Eisenberg, S. Büttner, C. Meisinger, G. Kroemer, F. Madeo, Apoptosis in yeast: triggers, pathways, subroutines, Cell Death Differ. 17 (5) (2010) 763–773.

[2] N. Guaragnella, M. Zdralević, L. Antonacci, S. Passarella, E. Marra, S. Giannattasio, The role of mitochondria in yeast programmed cell death, Front. Oncol. 2 (2012) 70.

[3] D.R. McIlwain, T. Berger, T.W. Mak, Caspase functions in cell death and disease, Cold Spring Harb. Perspect. Biol. 5 (4) (2013) a008656.

[4] S.E. Logue, S.J. Martin, Caspase activation cascades in apoptosis, Biochem. Soc. Trans. 36 (Pt 1) (2008) 1–9.

[5] F. Madeo, E. Herker, C. Maldener, S. Wissing, S. Lachelt, M. Herlan, M. Fehr, K. Lauber, S.J. Sigrist, S. Wesselborg, K.U. Frohlich, A caspase-related protease regulates apoptosis in yeast, Mol. Cell 9 (2002) 911–917.

[6] D. Wilkinson, M. Ramsdale, Proteases and caspase-like activity in the yeast *Saccharomyces cerevisiae*, Biochem. Soc. Trans. 39 (2011) 1502–1508.

[7] R.D. Silva, S. Manon, J. Gonçalves, L. Saraiva, M. Côrte-Real, The importance of humanized yeast to better understand the role of bcl-2 family in apoptosis: finding of novel therapeutic opportunities, Curr. Pharm. Des. 17 (3) (2011) 246–255 (Review).

[8] N. Watanabe, E. Lam, Two Arabidopsis metacaspases AtMCP1b and AtMCP2b are arginine/lysine-specific cysteine proteases and activate apoptosis-like cell death in yeast, J. Biol. Chem. 280 (2005) 14691–14699.

[9] L. Tsiatsiani, F. Van Breusegem, P. Gallois, A. Zavialov, E. Lam, P.V. Bozhkov, Metacaspases, Cell Death Differ. 18 (8) (2011) 1279–1288.

[10] A. Silva, B. Almeida, B. Sampaio-Marques, M.I. Reis, S. Ohlmeier, F. Rodrigues, Ad Vale, P. Ludovico, Glyceraldehyde-3-phosphate dehydrogenase (GAPDH) is a specific substrate of yeast metacaspase, Biochim. Biophys. Acta 1813 (12) (2011) 2044–2049.

[11] Q. Liang, W. Li, B. Zhou, Caspase-independent apoptosis in yeast, Biochim. Biophys. Acta 1783 (7) (2008) 1311–1319.

[12] C. Mazzoni, C. Falcone, Caspase-dependent apoptosis in yeast, Biochim. Biophys. Acta 1783 (7) (2008) 1320–1327.

[13] N. Guaragnella, L. Antonacci, S. Passarella, E. Marra, S. Giannattasio, Achievements and perspectives in yeast acetic acid-induced programmed cell death pathways, Biochem. Soc. Trans. 39 (5) (2011) 1538–1543.

[14] N. Guaragnella, C. Pereira, M.J. Sousa, L. Antonacci, S. Passarella, M. Corte-Real, E. Marra, S. Giannattasio, YCA1 participates in the acetic acid induced yeast programmed cell death also in a manner unrelated to its caspase like activity, FEBS Lett. 580 (30) (2006) 6880–6884.

[15] N. Guaragnella, A. Bobba, S. Passarella, E. Marra, S. Giannattasio, Yeast acetic acid-induced programmed cell death can occur without cytochrome c release which requires metacaspase YCA1, FEBS Lett. 584 (1) (2010) 224–228.

[16] R.E. Lee, L.G. Puente, M. Kaern, L.A. Megeney, A non-death role of the yeast metacaspase: Yca1p alters cell cycle dynamics, PLoS One 3 (8) (2008) e2956.

[17] S.M. Hill, X. Hao, B. Liu, T. Nyström, Life-span extension by a metacaspase in the yeast *Saccharomyces cerevisiae*, Science 344 (6190) (2014) 1389–1392.

[18] A. Shrestha, L.G. Puente, S. Brunette, L.A. Megeney, The role of Yca1 inproteostasis. Yca1 regulates the composition of the insoluble proteome, J. Proteomics 81 (2013) 24–30.

[19] M.A. Khan, P.B. Chock, E.R. Stadtman, Knockout of caspase-like gene, YCA1, abrogates apoptosis and elevates oxidized proteins in *Saccharomyces cerevisiae*, Proc. Natl. Acad. Sci. U. S. A. 102 (48) (2005) 17326–17331.

[20] S. Lefevre, D. Sliwa, F. Auchère, C. Brossas, C. Ruckenstuhl, N. Boggetto, E. Lesuisse, F. Madeo, J.M. Camadro, R. Santos, The yeast metacaspase is implicated in oxidative stress response in frataxin-deficient cells, FEBS Lett. 586 (2) (2012) 143–148.

[21] M. Ždralević, V. Longo, N. Guaragnella, S. Giannattasio, A.M. Timperio, L. Zolla, Differential proteome–metabolome profiling of YCA1-knock-out and wild type cells reveals novel metabolic pathways and cellular processes dependent on the yeast metacaspase, Mol. BioSyst. 11 (6) (2015) 1573–1583.

[22] F. Magherini, C. Tani, T. Gamberi, A. Caselli, L. Bianchi, L. Bini, A. Modesti, Protein expression profiles in *Saccharomyces cerevisiae* during apoptosis induced by H2O2, Proteomics 7 (9) (2007) 1434–1445.

[23] B. Almeida, S. Ohlmeier, A.J. Almeida, F. Madeo, C. Leao, F. Rodrigues, P. Ludovico, Yeast protein expression profile during acetic acid-induced apoptosis indicates causal involvement of the TOR pathway, Proteomics 9 (2009) 720–732.

[24] S. Giannattasio, A. Atlante, L. Antonacci, N. Guaragnella, P. Lattanzio, S. Passarella, E. Marra, Cytochrome c is released from coupled mitochondria of yeast en route to acetic acid-induced programmed cell death and can work as an electron donor and a ROS scavenger, FEBS Lett. 582 (10) (2008) 1519–1525.

[25] B. Westermann, W. Neupert, Mitochondria-targeted green fluorescent proteins: convenient tools for the study of organelle biogenesis in *Saccharomyces cerevisiae*, Yeast 16 (15) (2000 Nov) 1421–1427.

[26] D.C. Chen, B.C. Yang, T.T. Kuo, One-step transformation of yeast in stationary phase, Curr. Genet. 21 (1) (Jan 1992) 83–84.

[27] A. Shevchenko, M. Wilm, O. Vorm, M. Mann, Mass spectrometric sequencing of proteins silver-stained polyacrylamide gels, Anal. Chem. 68 (5) (1996) 850–858.

[28] R. Tautenhahn, G.J. Patti, E. Kalisiak, T. Miyamoto, M. Schmidt, F.Y. Lo, J. McBee, N.S. Baliga, G. Siuzdak, MetaXCMS: second-order analysis of untargeted metabolomics data, Anal. Chem. 83 (3) (2011) 696–700.

[29] E. Melamud, L. Vastag, J.D. Rabinowitz, Metabolomic analysis and visualization engine for LC–MS data, Anal. Chem. 82 (23) (2010) 9818–9826.

[30] C.A. Smith, G. O'Maille, E.J. Want, C. Qin, S.A. Trauger, T.R. Brandon, D.E. Custodio, R. Abagyan, G. Siuzdak, METLIN: a metabolite mass spectral database, Ther. Drug Monit. 27 (6) (2005) 747–751.

[31] P. Haussmann, F.K. Zimmermann, The role of mitochondria in carbon catabolite repression in yeast, Mol. Gen. Genet. 148 (2) (1976) 205–211.

[32] J.H. Kim, A. Roy, D. Jouandot II, K.H. Cho, The glucose signaling network in yeast, Biochim. Biophys. Acta 1830 (11) (2013) 5204–5210.

[33] G. Kispal, H. Steiner, D.A. Court, B. Rolinski, R. Lill, Mitochondrial and cytosolic branched-chain amino acid transaminases from yeast, homologs of the myc oncogene-regulated Eca39 protein, J. Biol. Chem. 271 (40) (1996) 24458–24464.

[34] K. Lecoq, I. Belloc, C. Desgranges, M. Konrad, B. Daignan-Fornier, YLR209c encodes *Saccharomyces cerevisiae* purine nucleoside phosphorylase, J. Bacteriol. 183 (16) (2001) 4910–4913.

[35] M.J. van Hemert, G.P. van Heusden, H.Y. Steensma, Yeast 14-3-3 proteins, Yeast 18 (10) (2001) 889–895.

[36] C. Wang, C. Skinner, E. Easlon, S.J. Lin, Deleting the 14-3-3 protein Bmh1 extends life span in *Saccharomyces cerevisiae* by increasing stress response, Genetics 183 (4) (2009) 1373–1384.

[37] Z. Xu, K. Graham, M. Foote, F. Liang, R. Rizkallah, M. Hurt, Y. Wang, Y. Wu, Y. Zhou, 14-3-3 protein targets misfolded chaperone-associated proteins to aggresomes, J. Cell Sci. 126 (Pt 18) (2013) 4173–4186.

[38] J. Reinders, A. Sickmann, Proteomics of yeast mitochondria, Methods Mol. Biol. 372 (2007) 543–557.

[39] R. Green, G. Lesage, A.M. Sdicu, P. Ménard, H. Bussey, A synthetic analysis of the *Saccharomyces cerevisiae* stress sensor Mid2p, and identification of a Mid2p-interacting protein, Zeo1p, that modulates the PKC1-MPK1 cell integrity pathway, Microbiology 149 (Pt 9) (2003) 2487–2499.

[40] E. Oxelmark, A. Marchini, I. Malanchi, F. Magherini, L. Jaquet, M.A. Hajibagheri, K.J. Blight, J.C. Jauniaux, M. Tommasino, Mmf1p, a novel yeast mitochondrial protein conserved throughout evolution and involved in maintenance of the mitochondrial genome, Mol. Cell. Biol. 20 (20) (2000) 7784–7797.

[41] J.M. Kim, H. Yoshikawa, K. Shirahige, A member of the YER057c/yjgf/Uk114 family links isoleucine biosynthesis and intact mitochondria maintenance in *Saccharomyces cerevisiae*, Genes Cells 6 (6) (2001) 507–517.

[42] N.M. Grüning, M. Rinnerthaler, K. Bluemlein, M. Mülleder, M.M. Wamelink, H. Lehrach, C. Jakobs, M. Breitenbach, M. Ralser, Pyruvate kinase triggers a metabolic feedback loop that controls redox metabolism in respiring cells, Cell Metab. 14 (3) (2011) 415–427.

[43] D. Thomas, Y. Surdin-Kerjan, Metabolism of sulfur amino acids in *Saccharomyces cerevisiae*, Microbiol. Mol. Biol. Rev. 61 (4) (1997) 503–532 (Review).

[44] D.G. Smethurst, I.W. Dawes, C.W. Gourlay, Actin — a biosensor that determines cell fate in yeasts, FEMS Yeast Res. 14 (1) (2014) 89–95.

[45] A.L. Hughes, D.E. Gottschling, An early age increase in vacuolar pH limits mitochondrial function and lifespan in yeast, Nature 492 (7428) (2012) 261–265.

[46] C.E. Zeller, S.C. Parnell, H.G. Dohlman, The RACK1 ortholog Asc1 functions as a G-protein beta subunit coupled to glucose responsiveness in yeast, J. Biol. Chem. 282 (34) (2007) 25168–25176.

[47] V.R. Gerbasi, C.M. Weaver, S. Shrestha, D.B. Friedman, A.J. Link, Yeast Asc1p and mammalian RACK1 are functionally orthologous core 40S ribosomal proteins that repress gene expression, Mol. Cell. Biol. 24 (18) (2004) 8276–8287.

[48] F. Wieland, E.A. Siess, L. Renner, C. Verfürth, F. Lynen, Distribution of yeast fatty acid synthetase subunits: three-dimensional model of the enzyme, Proc. Natl. Acad. Sci. U. S. A. 75 (12) (1978) 5792–5796.

[49] S.J. Kolodziej, P.A. Penczek, J.P. Schroeter, J.K. Stoops, Structure-function relationships of the *Saccharomyces cerevisiae* fatty acid synthase. Three-dimensional structure, J. Biol. Chem. 271 (45) (1996) 28422–28429.

[50] M. Leibundgut, S. Jenni, C. Frick, N. Ban, Structural basis for substrate delivery by acyl carrier protein in the yeast fatty acid synthase, Science 316 (5822) (2007) 288–290.

[51] I.B. Lomakin, Y. Xiong, T.A. Steitz, The crystal structure of yeast fatty acid synthase, a cellular machine with eight active sites working together, Cell 129 (2) (2007) 319–332.

[52] S.D. Kohlwein, S. Eder, C.S. Oh, C.E. Martin, K. Gable, D. Bacikova, T. Dunn, Tsc13p is required for fatty acid elongation and localizes to a novel structure at the nuclear-vacuolar interface in *Saccharomyces cerevisiae*, Mol. Cell. Biol. 21 (1) (Jan 2001) 109–125.

[53] P. Spincemaille, N. Matmati, Y.A. Hannun, B.P. Cammue, K. Thevissen, Sphingolipids and mitochondrial function in budding yeast, Biochim. Biophys. Acta 1840 (10) (2014) 3131–3137.

[54] A. Rego, M. Costa, S.R. Chaves, N. Matmati, H. Pereira, M.J. Sousa, P. Moradas-Ferreira, Y.A. Hannun, V. Costa, M. Côrte-Real, Modulation of mitochondrial outer membrane permeabilization and apoptosis by ceramide metabolism, PLoS One 7 (11) (2012) e48571.

[55] B. Westermann, Bioenergetic role of mitochondrial fusion and fission, Biochim. Biophys. Acta 1817 (10) (2012) 1833–1838.

[56] Y. Fannjiang, W.C. Cheng, S.J. Lee, B. Qi, J. Pevsner, J.M. McCaffery, R.B. Hill, G. Basañez, J.M. Hardwick, Mitochondrial fission proteins regulate programmed cell death in yeast, Genes Dev. 18 (2004) 2785–2797.

[57] C. Pereira, S. Chaves, S. Alves, B. Salin, N. Camougrand, S. Manon, M.J. Sousa, M. Corte-Real, Mitochondrial degradation in acetic acid-induced yeast apoptosis: the role of Pep4 and the ADP/ATP carrier, Mol. Microbiol. 76 (6) (2010) 1398–1410.

[58] J.M. Hardwick, W.C. Cheng, Mitochondrial programmed cell death pathways in yeast, Dev. Cell 7 (5) (2004) 630–632.

[59] M. Muller, K. Lu, A.S. Reichert, Mitophagy and mitochondrial dynamics in *Saccharomyces cerevisiae*, Biochim. Biophys. Acta (2015)http://dx.doi.org/10.1016/j.bbamcr.2015.02.024 (S0167-4889(15)00074-9).

[60] M.J. Sousa, F. Azevedo, A. Pedras, C. Marques, O.P. Coutinho, A. Preto, H. Geros, S.R. Chaves, M. Corte-Real, Vacuole-mitochondrial cross-talk during apoptosis in yeast:

a model for understanding lysosome–mitochondria-mediated apoptosis in mammals, Biochem. Soc. Trans. 39 (5) (2011) 1533–1537.
[61] X. Wang, The expanding role of mitochondria in apoptosis, Genes Dev. 15 (22) (Nov 15 2001) 2922–2933 (Review, PubMed PMID: 11711427).
[62] F. Madeo, D. Carmona-Gutierrez, J. Ring, S. Büttner, T. Eisenberg, G. Kroemer, Caspase-dependent and caspase-independent cell death pathways in yeast, Biochem. Biophys. Res. Commun. 382 (2009) 227–231.
[63] A. Fico, F. Paglialunga, L. Cigliano, P. Abrescia, P. Verde, G. Martini, I. Iaccarino, S. Filosa, Glucose-6-phosphate dehydrogenase plays a crucial role in protection from redox-stress-induced apoptosis, Cell Death Differ. 11 (2004) 823–831.
[64] M.L. Circu, T.Y. Aw, Glutathione and apoptosis, Free Radic. Res. 42 (8) (2008) 689–706.
[65] S. Wissing, P. Ludovico, E. Herker, S. Büttner, S.M. Engelhardt, T. Decker, A. Link, A. Proksch, F. Rodrigues, M. Corte-Real, K.U. Fröhlich, J. Manns, C. Candé, S.J. Sigrist, G. Kroemer, F. Madeo, An AIF orthologue regulates apoptosis in yeast, J. Cell Biol. 166 (7) (2004) 969–974.
[66] Y. Ohya, N. Umemoto, I. Tanida, A. Ohta, H. Iida, Y. Anraku, Calcium-sensitive cls mutants of *Saccharomyces cerevisiae* showing a Pet-phenotype are ascribable to defects of vacuolar membrane H(+)-ATPase activity, J. Biol. Chem. 266 (21) (1991) 13971–13977.
[67] M. Ralser, M.M. Wamelink, A. Kowald, B. Gerisch, G. Heeren, E.A. Struys, E. Klipp, C. Jakobs, M. Breitenbach, H. Lehrach, S. Krobitsch, Dynamic rerouting of the carbohydrate flux is key to counteracting oxidative stress, J. Biol. 6 (4) (2007) 10 (21).
[68] B.J. Altman, J.C. Rathmell, Metabolic stress in autophagy and cell death pathways, Cold Spring Harb. Perspect. Biol. (2012)http://dx.doi.org/10.1101/cshperspect.a008763. Review.
[69] W. Seufert, S. Jentsch, Yeast ubiquitin-conjugating enzymes involved in selective protein degradation are essential for cell viability, Acta Biol. Hung. 42 (1–3) (1991) 27–37 (Review).
[70] S.M. Chuang, K. Madura, *Saccharomyces cerevisiae* Ub-conjugating enzyme Ubc4 binds the proteasome in the presence of translationally damaged proteins, Genetics 171 (4) (2005) 1477–1484.
[71] D. Valenti, R.A. Vacca, N. Guaragnella, S. Passarella, E. Marra, S. Giannattasio, A transient proteasome activation is needed for acetic acid-induced programmed cell death to occur in *Saccharomyces cerevisiae*, FEMS Yeast Res. 8 (3) (2008) 400–404.
[72] S.H. Lecker, A.L. Goldberg, W.E. Mitch, Protein degradation by the ubiquitin–proteasome pathway in normal and disease states, J. Am. Soc. Nephrol. 17 (7) (2006) 1807–1819.
[73] G.M. Jenkins, A. Richards, T. Wahl, C. Mao, L. Obeid, Y. Hannun, Involvement of yeast sphingolipids in the heat stress response of *Saccharomyces cerevisiae*, J. Biol. Chem. 272 (1997) 32566–32572.
[74] G.B. Wells, R.C. Dickson, R.L. Lester, Heat-induced elevation of ceramide in *Saccharomyces cerevisiae* via de novo synthesis, J. Biol. Chem. 273 (1998) 7235–7243.
[75] L.J. Siskind, M. Colombini, The lipids C2- and C16-ceramide form large stable channels. Implications for apoptosis, J. Biol. Chem. 275 (2000) 38640–38644.
[76] M.N. Perera, V. Ganesan, L.J. Siskind, Z.M. Szulc, J. Bielawski, A. Bielawska, R. Bittman, M. Colombini, Ceramide channels: influence of molecular structure on channel formation in membranes, Biochim. Biophys. Acta 1818 (2012) 1291–1301.
[77] D. Carmona-Gutierrez, A. Reisenbichler, P. Heimbucher, M.A. Bauer, R.J. Braun, C. Ruckenstuhl, S. Büttner, T. Eisenberg, P. Rockenfeller, K.U. Fröhlich, G. Kroemer, F. Madeo, Ceramide triggers metacaspase-independent mitochondrial cell death in yeast, Cell Cycle 10 (22) (2011) 3973–3978.
[78] B. Ogretmen, Y.A. Hannun, Biologically active sphingolipids in cancer pathogenesis and treatment, Nat. Rev. Cancer 4 (2004) 604–616.
[79] L.M. Knowles, C. Yang, A. Osterman, J.W. Smith, Inhibition of fatty-acid synthase induces caspase-8-mediated tumor cell apoptosis by up-regulating DDIT4, J. Biol. Chem. 283 (46) (2008) 31378–31384.
[80] S. Bandyopadhyay, R. Zhan, Y. Wang, S.K. Pai, S. Hirota, S. Hosobe, Y. Takano, K. Saito, E. Furuta, M. Iiizumi, S. Mohinta, M. Watabe, C. Chalfant, K. Watabe, Mechanism of apoptosis induced by the inhibition of fatty acid synthase in breast cancer cells, Cancer Res. 66 (11) (2006) 5934–5940.
[81] S. Giannattasio, N. Guaragnella, A.A. Arbini, L. Moro, Stress-related mitochondrial components and mitochondrial genome as targets of anticancer therapy, Chem. Biol. Drug Des. 81 (1) (2013) 102–112.
[82] N. Guaragnella, V. Palermo, A. Galli, L. Moro, C. Mazzoni, S. Giannattasio, The expanding role of yeast in cancer research and diagnosis: insights into the function of the oncosuppressors p53 and BRCA1/2, FEMS Yeast Res. 14 (1) (2014) 2–16.